Institute for Theoretical Physics

Collaborative Research Center TRR 257
Particle Physics Phenomenology after the Higgs Discovery

Karlsruher Institut für Technologie

Complete Next-to-Leading-Order QCD corrections to ZZ production through gluon fusion

High Precision for Hard Processes (HP2 2024)

Bakul Agarwal, Karlsruhe Institute of Technology (with Stephen Jones, Matthias Kerner, and Andreas von Manteuffel)

Based on https://arxiv.org/abs/2011.15113 and https://arxiv.org/abs/2404.05684

Motivation

Precision measurements:

Background to Higgs production through gluon fusion [CMS 2018] [ATLAS 2020]

Higgs Width:

Indirect constraints on Higgs width through off-shell Higgs production [ATLAS 2018] [CMS 2019] [Caola, Melnikov 2013] [Campbell, Ellis, Williams 2013]

Motivation

Karlsruher Institut für Technologie

Precision measurements:

Background to Higgs production through gluon fusion [CMS 2018] [ATLAS 2020]

Higgs Width:

Indirect constraints on Higgs width through off-shell Higgs production [ATLAS 2018] [CMS 2019] [Caola, Melnikov 2013] [Campbell, Ellis, Williams 2013]

BSM searches:

Searches for heavy diboson resonances decaying to 4 lepton final states [ATLAS 2020] [CMS 2023]

Anomalous couplings:

Constrain anomalous $t\bar{t}Z$, triple gauge couplings [ATLAS 2023]

Motivation

$gg \to ZZ$ at the LHC:

Loop induced; formally NNLO for $pp \to ZZ$ (starting at $O(\alpha_S^2)$)

Large contribution due to high gluon luminosity; $\sim 60\,\%$ of the total NNLO correction [Cascioli, Gehrmann, Grazzini, Kallweit, Maierhöfer, von Manteuffel, Pozzorini, Rathlev, Tancredi, Weihs (2014)]

$gg \to ZZ$ at NLO (massless quarks in the loop) increases total $pp \to ZZ$ by ~ 5%
[Grazzini, Kallweit, Wiesemann, Yook (2018)]

Top quark effects expected to be significant, especially for longitudinal modes due to Goldstone boson equivalence theorem

$\Longrightarrow$ Need a full NLO calculation

NLO Calculation

Next-to-Leading Order cross-section:

$$\mathrm{d}\sigma_{NLO} = \mathrm{d}\sigma_B + \mathrm{d}\sigma_V + \mathrm{d}\sigma_R$$

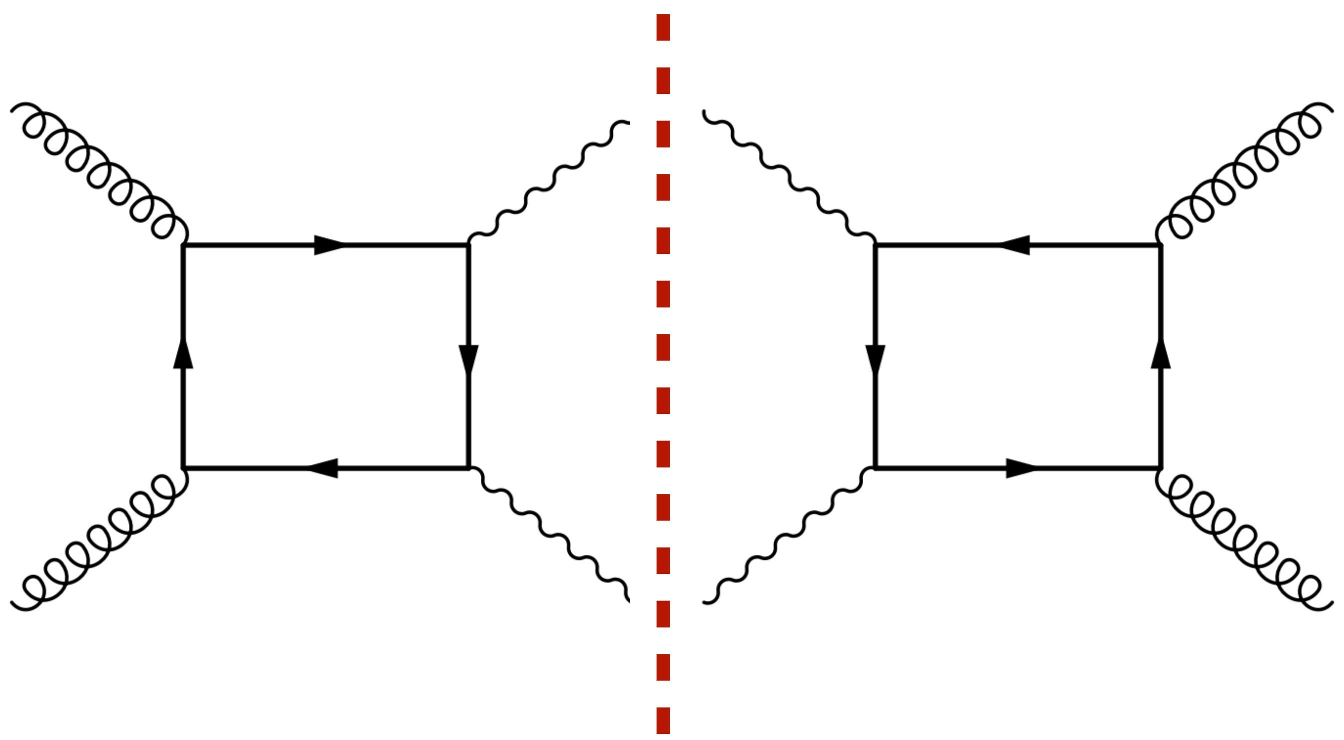

Born

$2 \rightarrow 2$ amplitude
at 1-loop

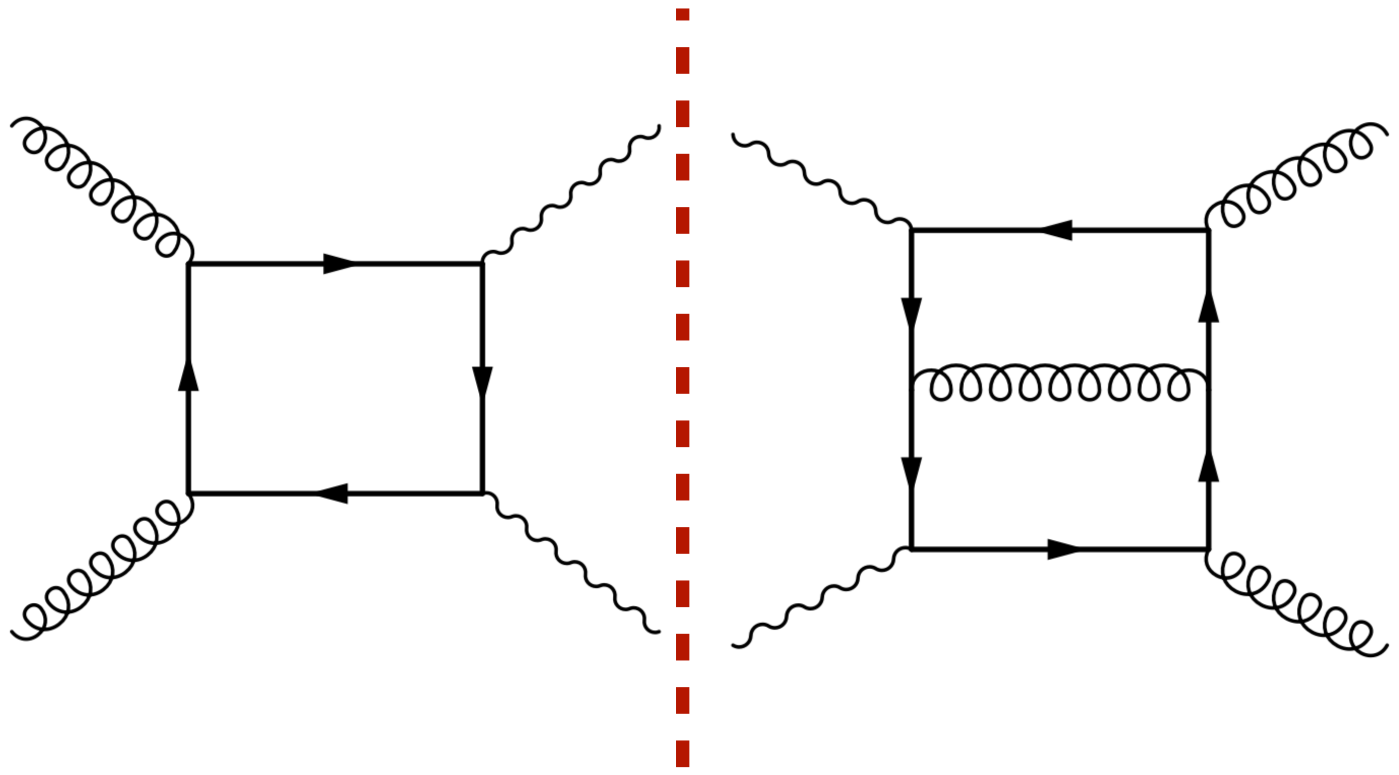

Virtuals

$2 \rightarrow 2$ amplitude
at 2-loops

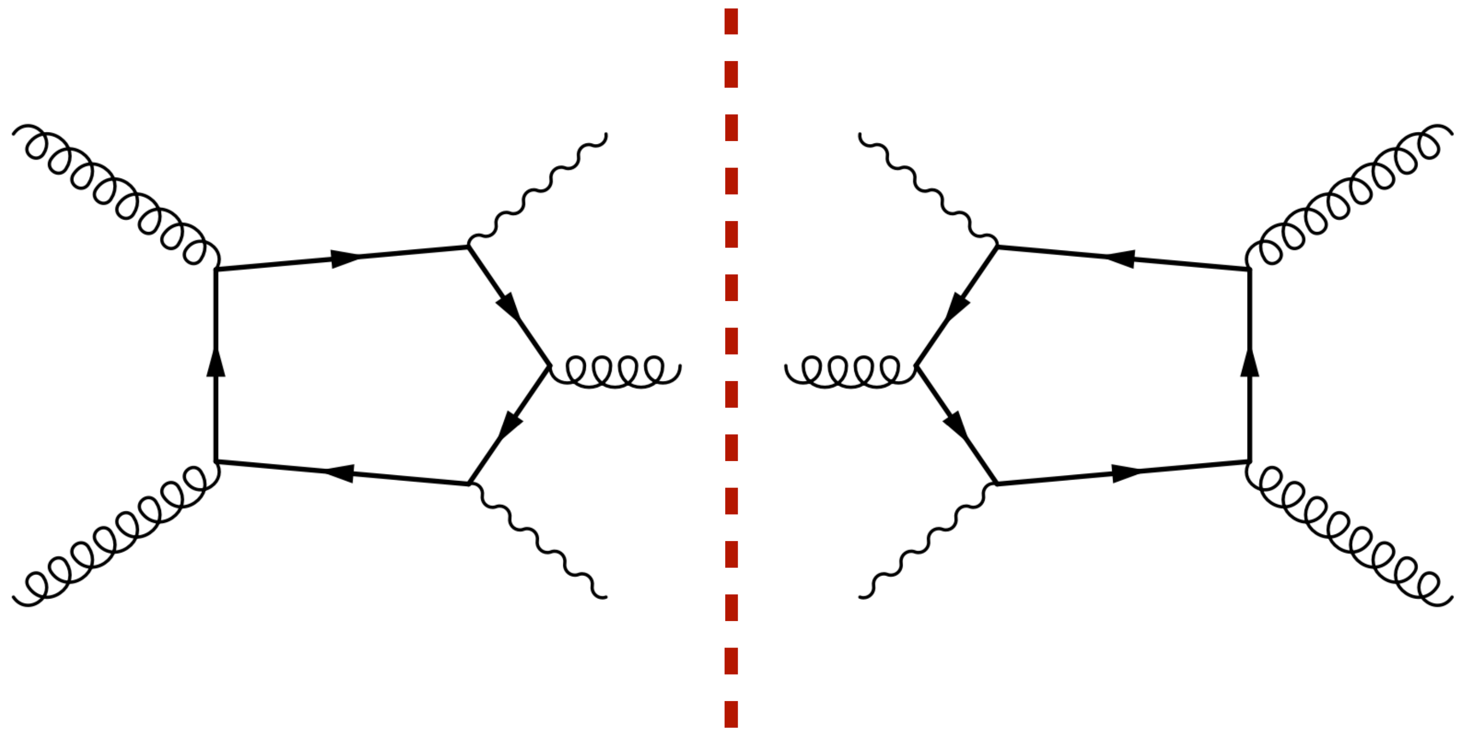

Reals

$2 \rightarrow 3$ amplitude
at 1-loop

NLO Calculation

Next-to-Leading Order cross-section:

$$\mathrm{d}\sigma_{NLO} = \mathrm{d}\sigma_B + \mathrm{d}\sigma_V + \mathrm{d}\sigma_R$$

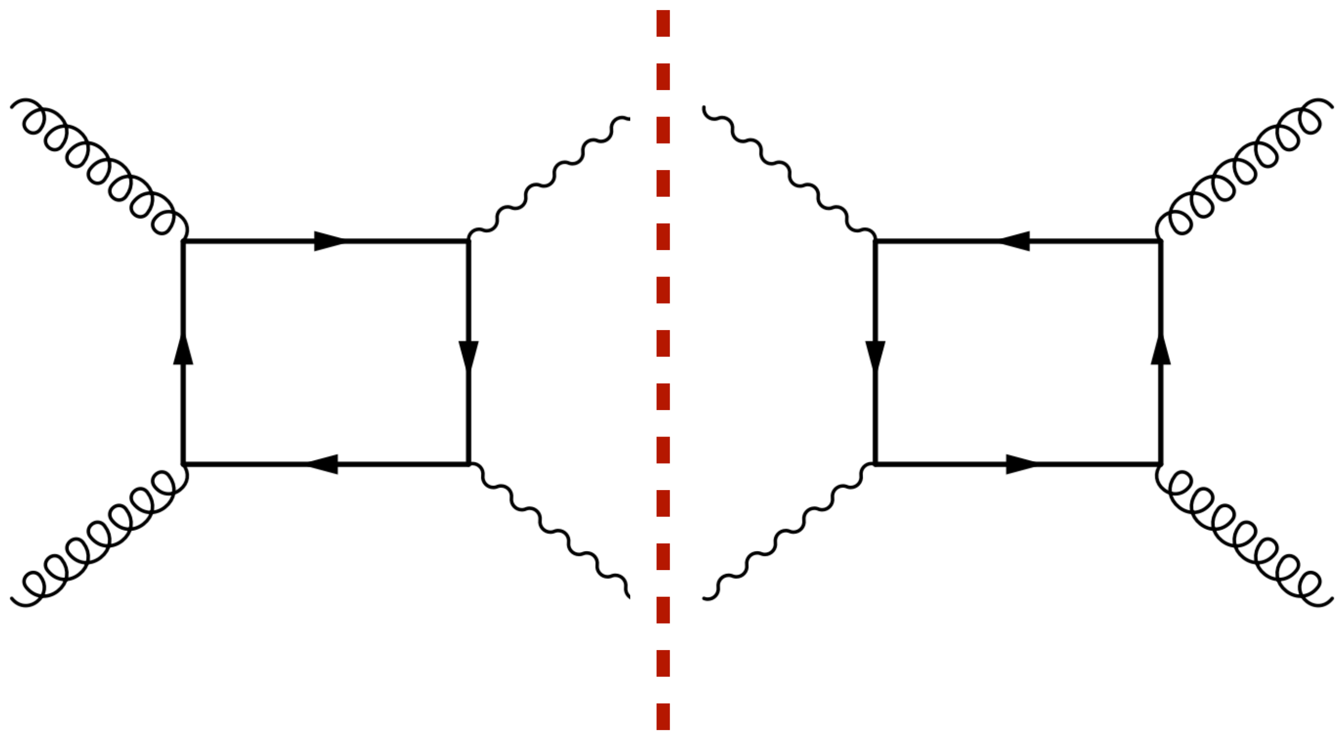

Born

$2 \rightarrow 2$ amplitude at 1-loop

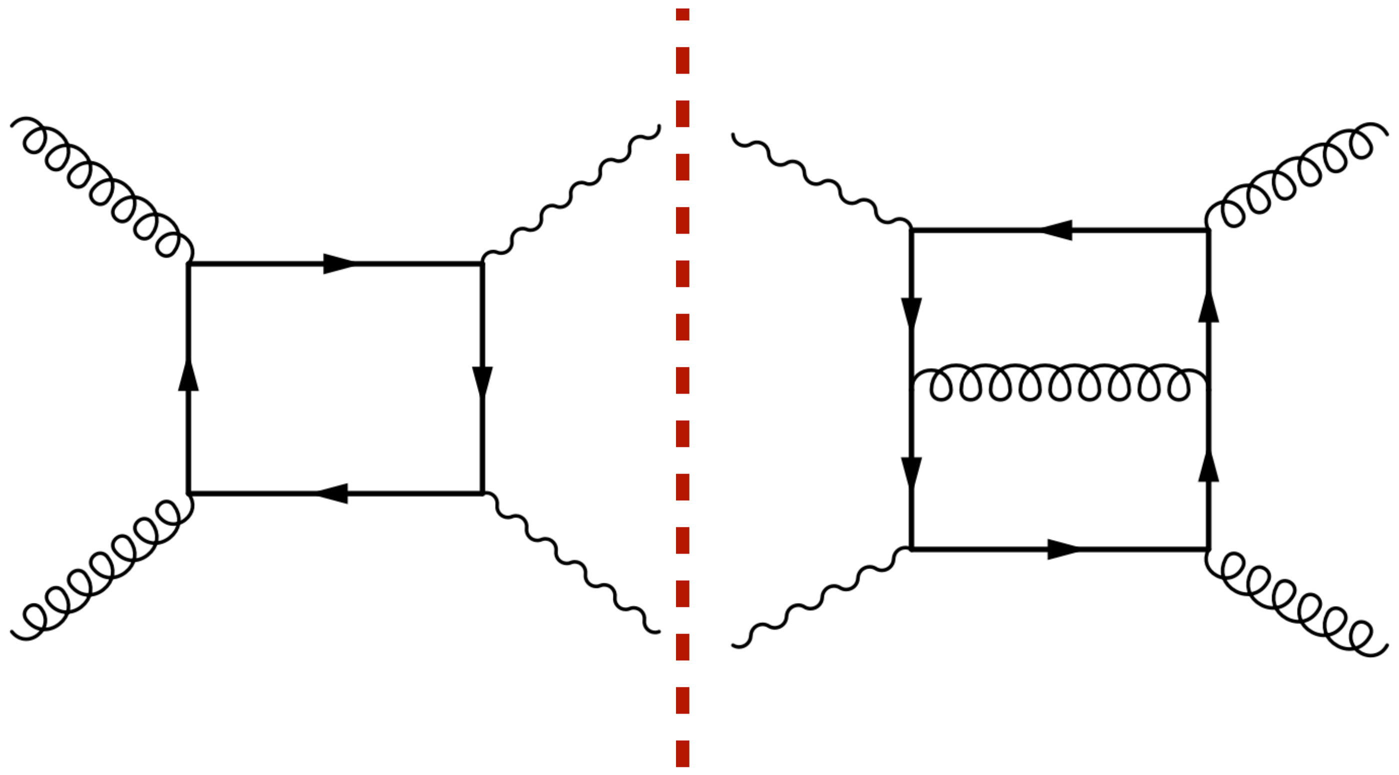

Virtuals

$2 \rightarrow 2$ amplitude at 2-loops

Conceptually challenging

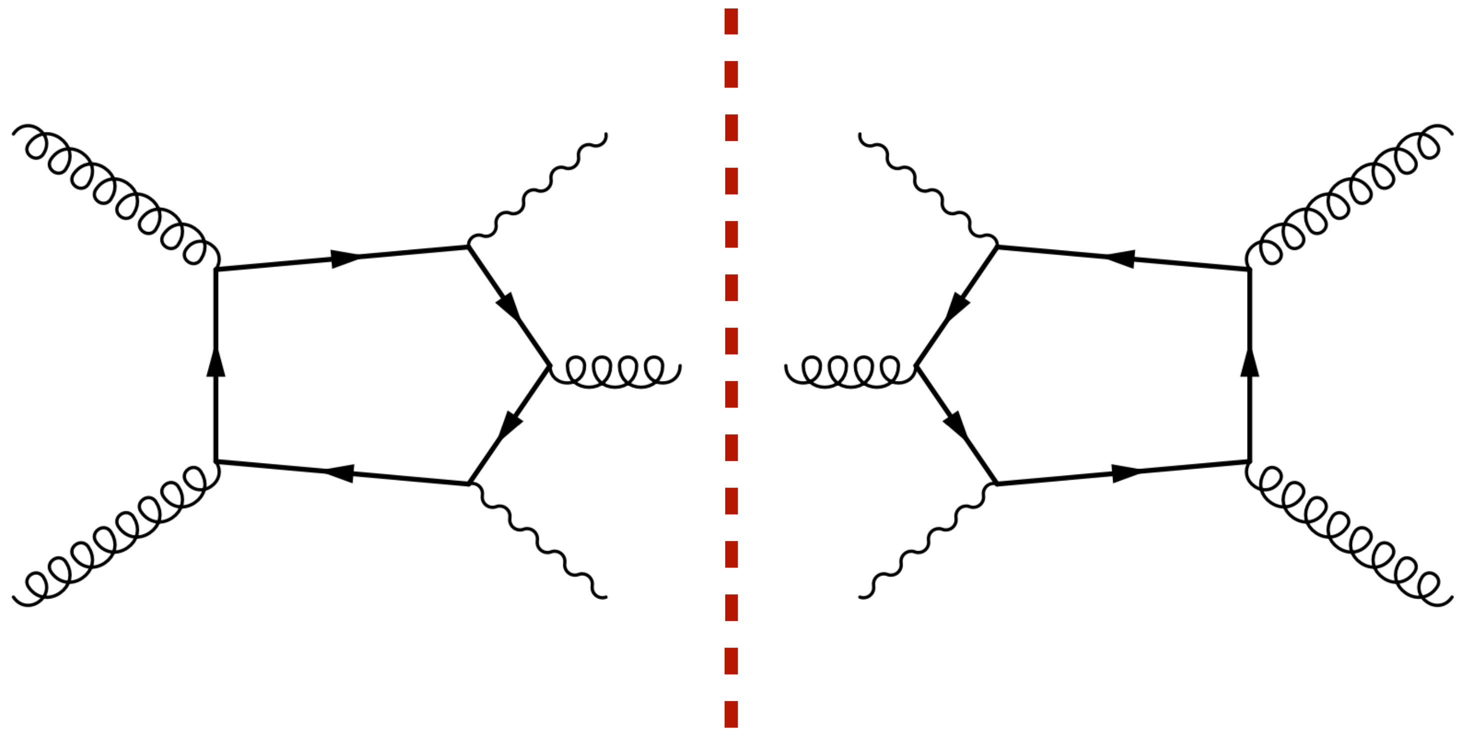

Reals

$2 \rightarrow 3$ amplitude at 1-loop

NLO Calculation

Next-to-Leading Order cross-section:

$$\mathrm{d}\sigma_{NLO} = \mathrm{d}\sigma_B + \mathrm{d}\sigma_V + \mathrm{d}\sigma_R$$

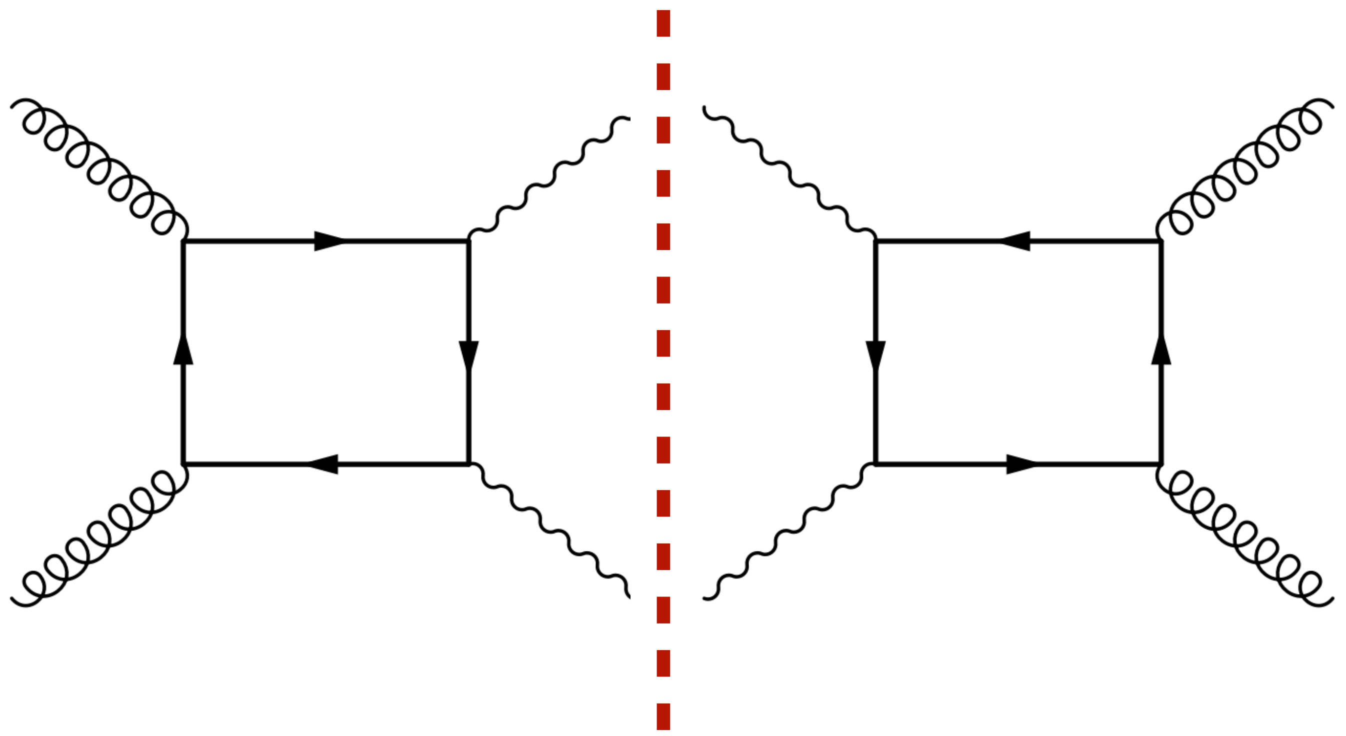

Born

$2 \rightarrow 2$ amplitude
at 1-loop

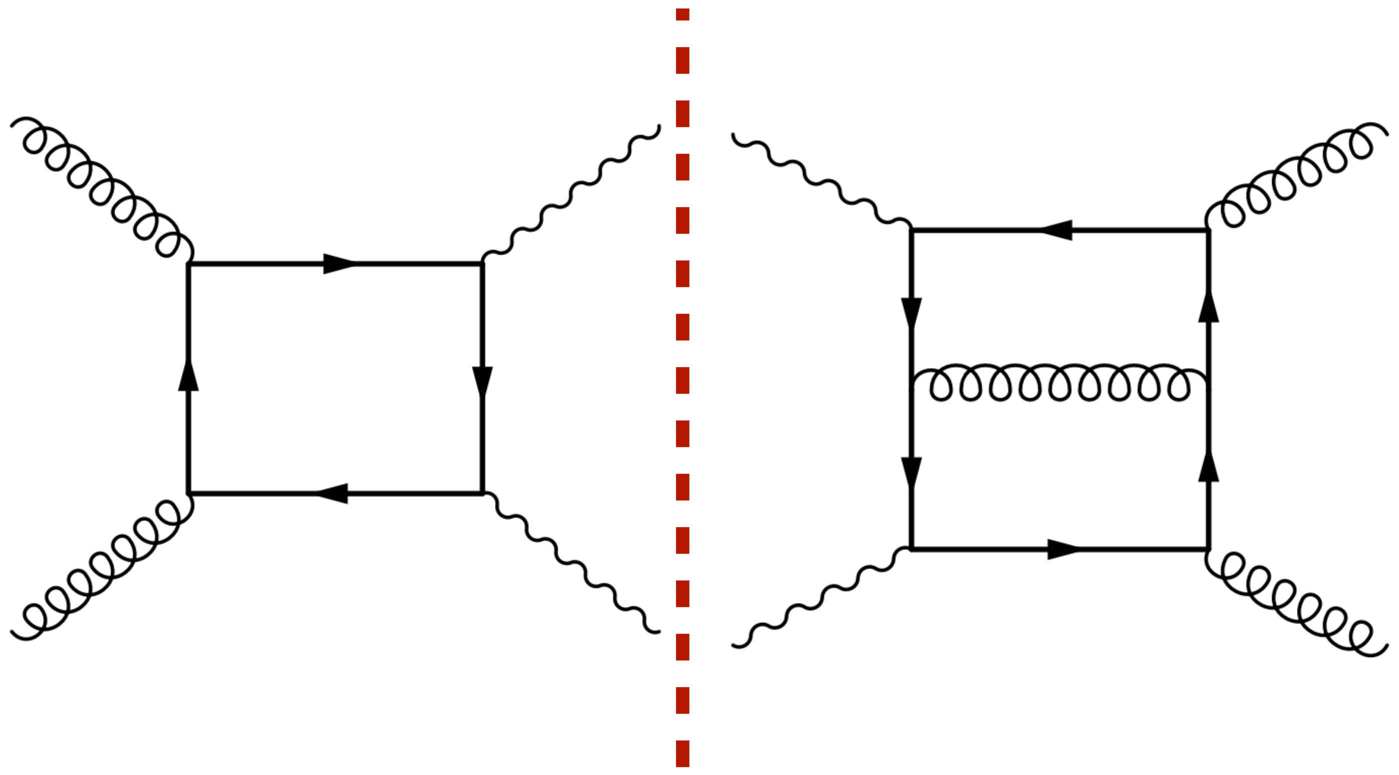

Virtuals

$2 \rightarrow 2$ amplitude
at 2-loops

Conceptually challenging

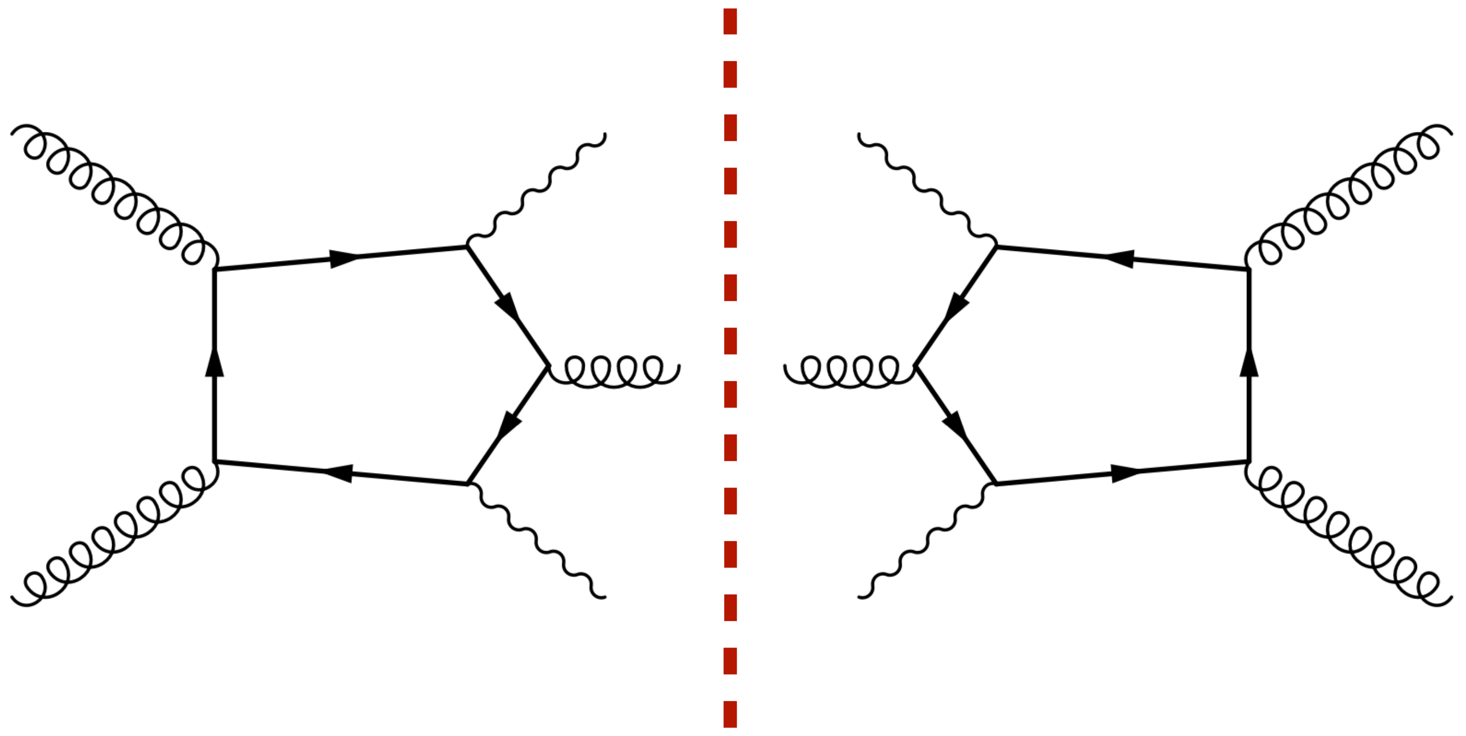

Reals

$2 \rightarrow 3$ amplitude
at 1-loop

Numerically challenging

Two-loop Amplitude

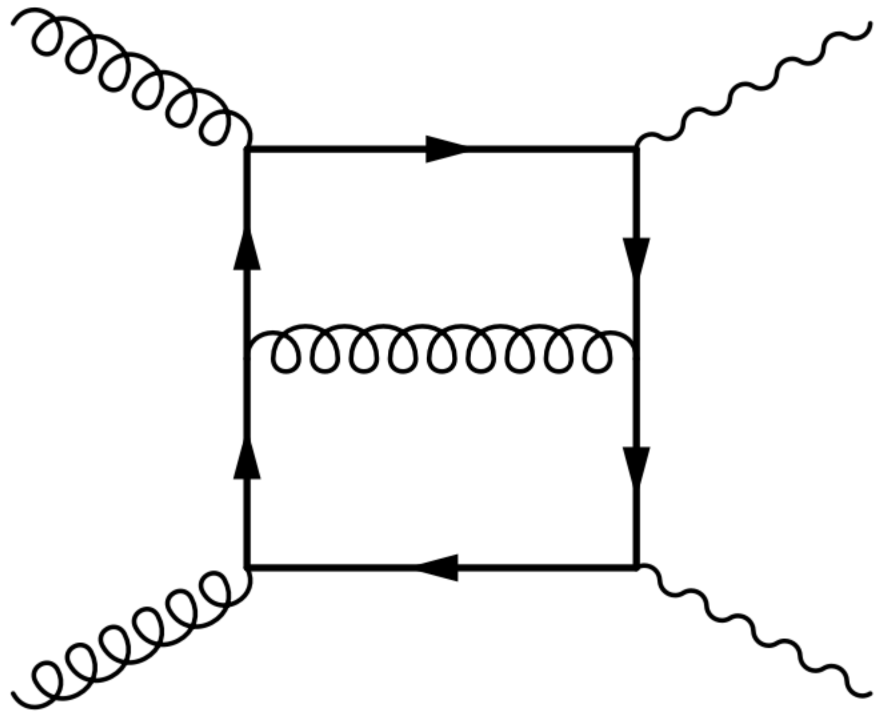

Massless quarks $(\mathbf{A_l})$

[von Manteuffel, Tancredi (2015)]
[Caola, Henn, Melnikov, Smirnov, Smirnov (2015)]

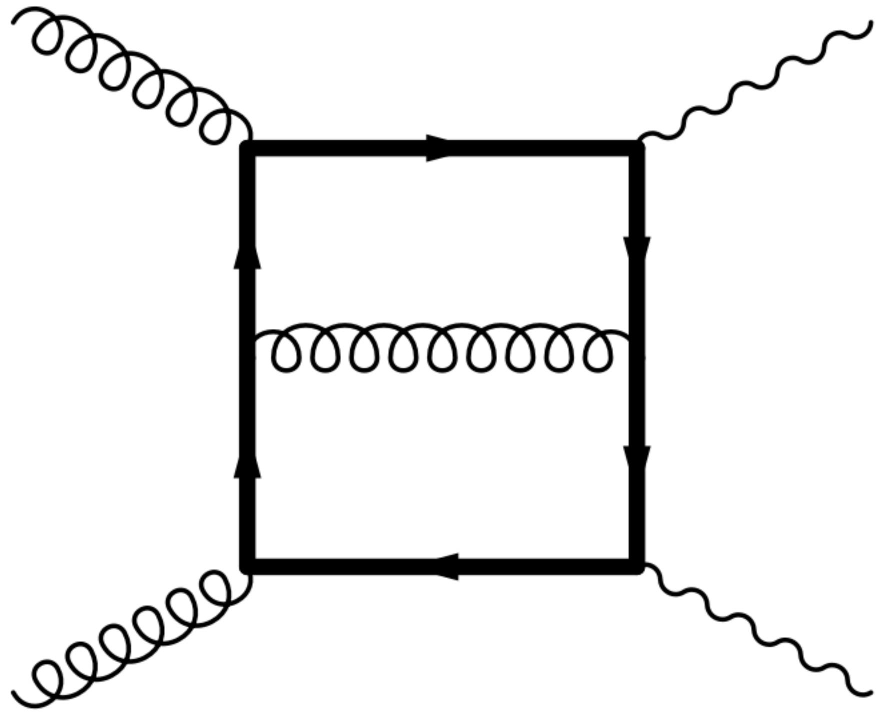

Massive $(\mathbf{A_h})$

[BA, Jones, von Manteuffel (2020)]
[Brønnum-Hansen, Wang (2021)]

And for various expansions: [Melnikov, Dowling (2015)] [Caola et al (2016)] [Cambell, Ellis, Czakon, Kirchner (2016)] [Gröber, Maier, Rauh (2019)] [Davies, Mishima, Steinhauser, Wellmann (2020)]

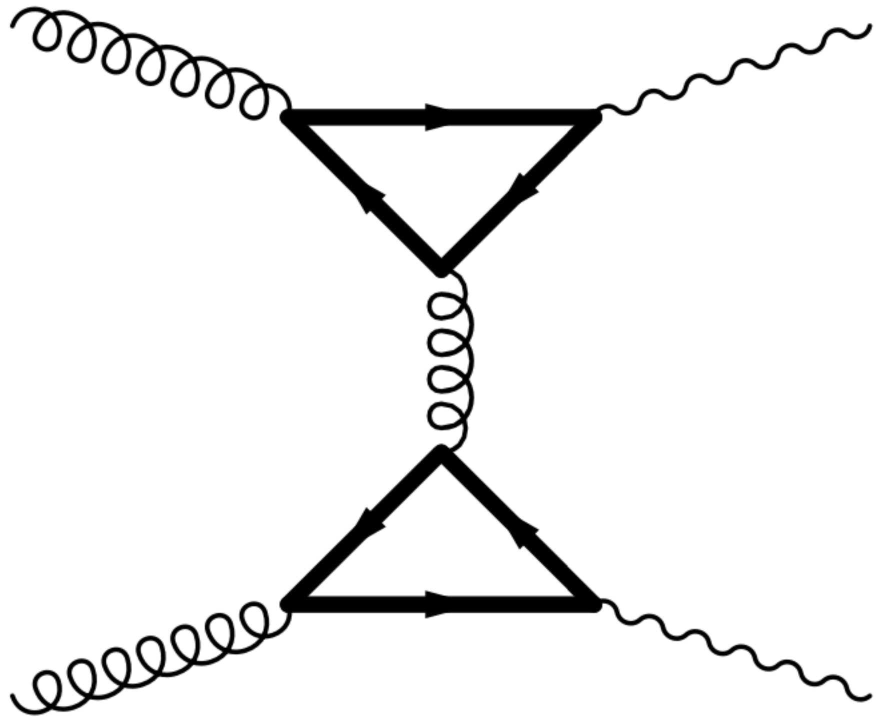

Anomaly type $(\mathbf{B})$

[Kniehl, Kühn (1990)] [Cambell, Ellis, Zanderighi (2007)] [Cambell, Ellis, Czakon, Kirchner (2016)]

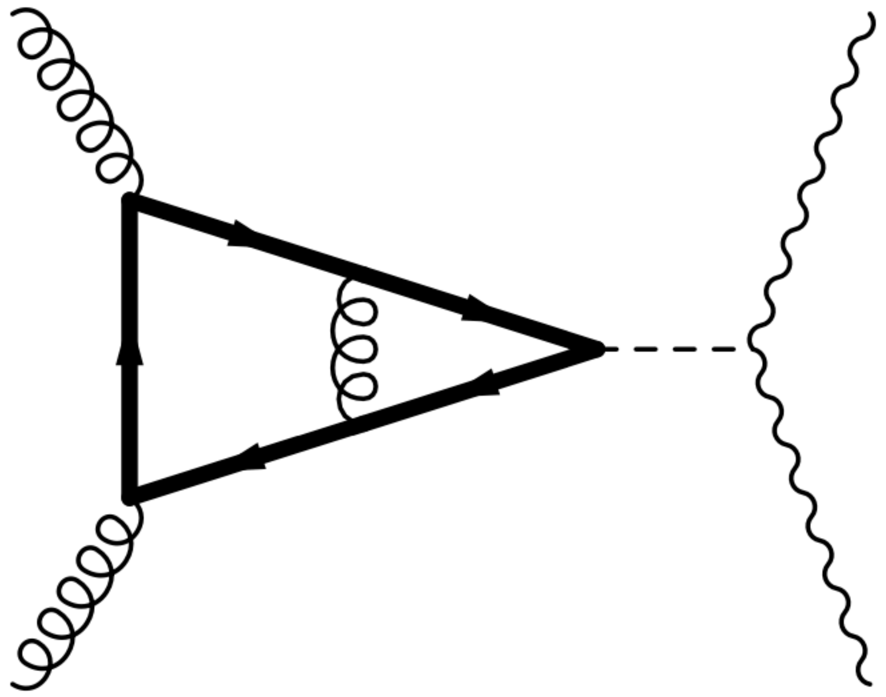

Higgs mediated $(\mathbf{C})$

[Spira et al (1995)] [Harlander & Kant (2005)] [Anastasiou et al (2006)] [Bonciani et al (2006)]

Two-loop Amplitude

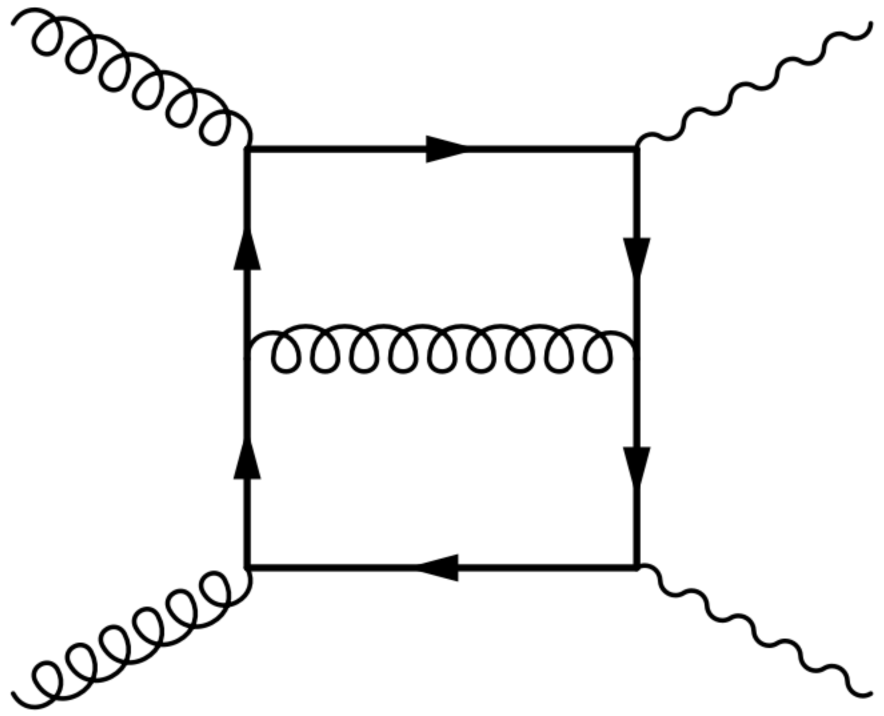

Massless quarks $(\mathbf{A_l})$

[von Manteuffel, Tancredi (2015)]
[Caola, Henn, Melnikov, Smirnov, Smirnov (2015)]

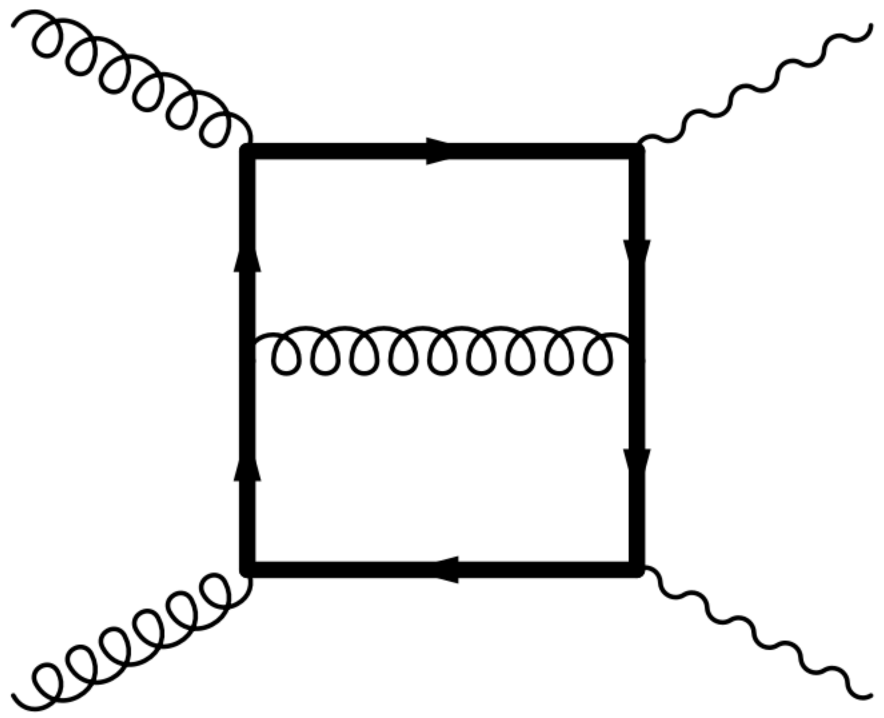

Massive $(\mathbf{A_h})$

[BA, Jones, von Manteuffel (2020)]
[Brønnum-Hansen, Wang (2021)]

And for various expansions: [Melnikov, Dowling (2015)] [Caola et al (2016)] [Cambell, Ellis, Czakon, Kirchner (2016)] [Gröber, Maier, Rauh (2019)] [Davies, Mishima, Steinhauser, Wellmann (2020)]

Also see Ramona's talk

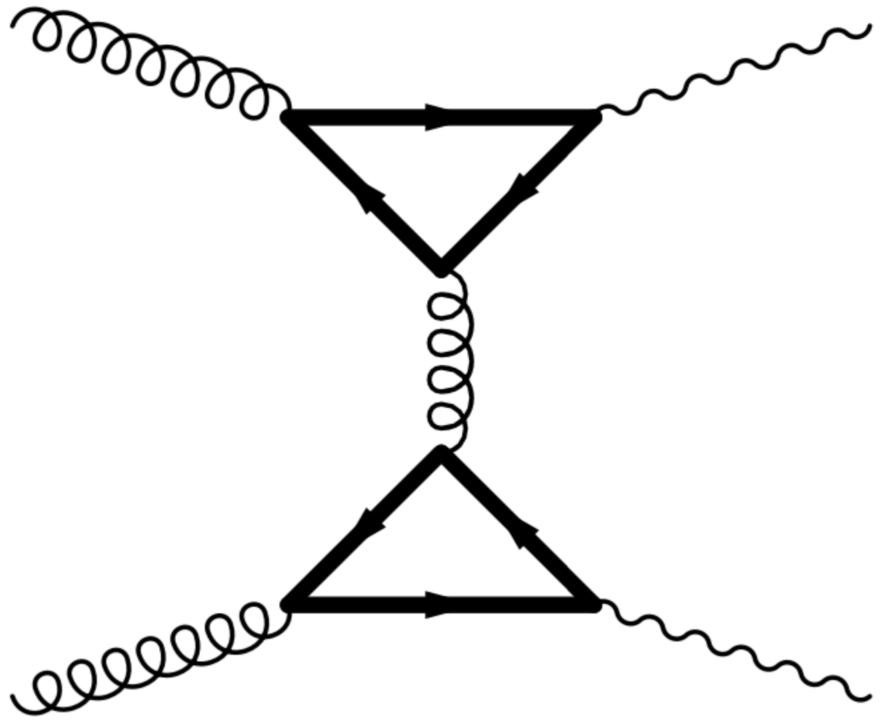

Anomaly type $(\mathbf{B})$

[Kniehl, Kühn (1990)]
[Cambell, Ellis, Zanderighi (2007)] [Cambell, Ellis, Czakon, Kirchner (2016)]

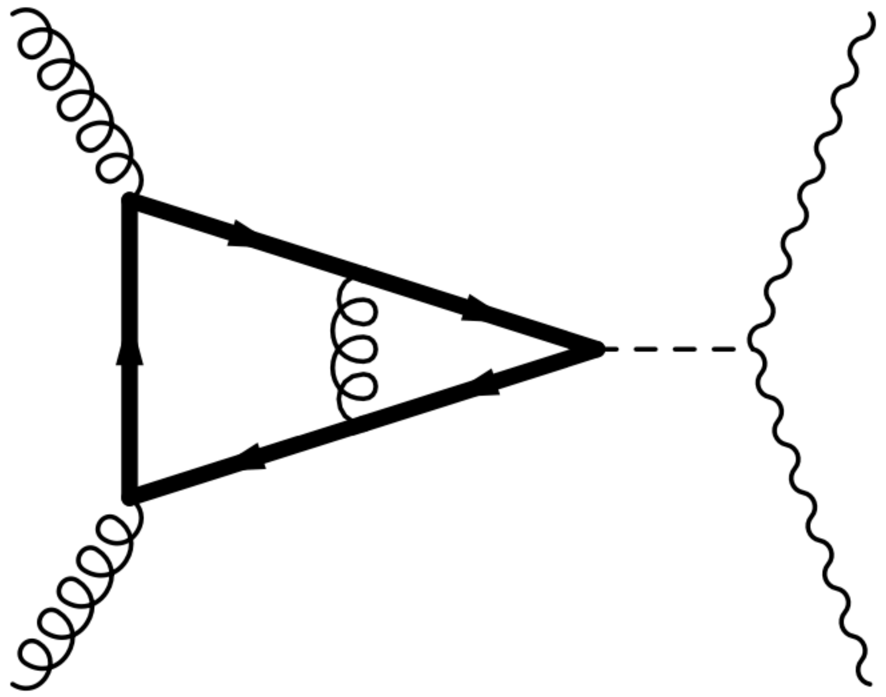

Higgs mediated $(\mathbf{C})$

[Spira et al (1995)] [Harlander & Kant (2005)] [Anastasiou et al (2006)] [Bonciani et al (2006)]

Results

Karlsruher Institut für Technologie

Write the UV and IR finite amplitudes (after UV renormalisation and IR subtraction respectively) as:

$$\mathcal{M}^{fin}_{\lambda_1\lambda_2\lambda_3\lambda_4} = \left(\frac{\alpha_S}{2\pi}\right)\mathcal{M}^{(1)}_{\lambda_1\lambda_2\lambda_3\lambda_4} + \left(\frac{\alpha_S}{2\pi}\right)^2\mathcal{M}^{(2)}_{\lambda_1\lambda_2\lambda_3\lambda_4} + O\left(\alpha_S\right)^3$$

Define 1-loop squared and interference between 1-loop and 2-loop amplitudes:

$$\mathcal{V}^{(1)}_{\lambda_1\lambda_2\lambda_3\lambda_4} = |\,\mathcal{M}^{(1)}_{\lambda_1\lambda_2\lambda_3\lambda_4}\,|^2$$

$$\mathcal{V}^{(2)}_{\lambda_1\lambda_2\lambda_3\lambda_4} = 2\,\mathrm{Re}\left(\mathcal{M}^{*(1)}_{\lambda_1\lambda_2\lambda_3\lambda_4}\mathcal{M}^{(2)}_{\lambda_1\lambda_2\lambda_3\lambda_4}\right)$$

Note that in the following results, only the pure top-quark contributions are included (i.e. no Higgs mediated diagrams or massless internal quarks)

Numerical Evaluation

Karlsruher Institut für Technologie

Integration strategy

Helicity amplitudes $\mathscr{M}^{(2)}_{\lambda_1\lambda_2\lambda_3\lambda_4}$ written as a linear combination of $\sim O(10^4)$ integrals after sector decomposition i.e. each sector of a master integral is considered and evaluated separately

Number of evaluations for each integral set dynamically to minimise the evaluation time for $\mathscr{M}^{(2)}_{\lambda_1\lambda_2\lambda_3\lambda_4}$ instead of each integral [Borowka et al (2016)]

$$T = \Sigma\, t_i \;+\; \lambda\,(\sigma^2 - \Sigma_i\, \sigma_i^2)$$

T : Total integration time
t_j : Integration time for integral j
σ : Required precision
σ_i : Estimated precision for integral i
λ : Lagrange Multiplier

Quasi-Monte Carlo algorithm for quadrature [Li, Wang, Zhao (2015)] [Borowka et al (2017)]

Request per-cent precision on each helicity amplitude (and ~10% on form factors A_i); much better precision obtained usually

Numerical Evaluation

Use the born calculation (with only top quarks) to generate unweighted events to sample the virtual corrections (~3000 points)

Good numerical stability in most regions of phase space, in particular around the top-quark threshold

Runtimes in $O(10)$ min for large part of the phase space with expected difficulties for $|cos\theta| \sim 1$ (very small p_T)

Better than per-mille precision for most of the phase-space

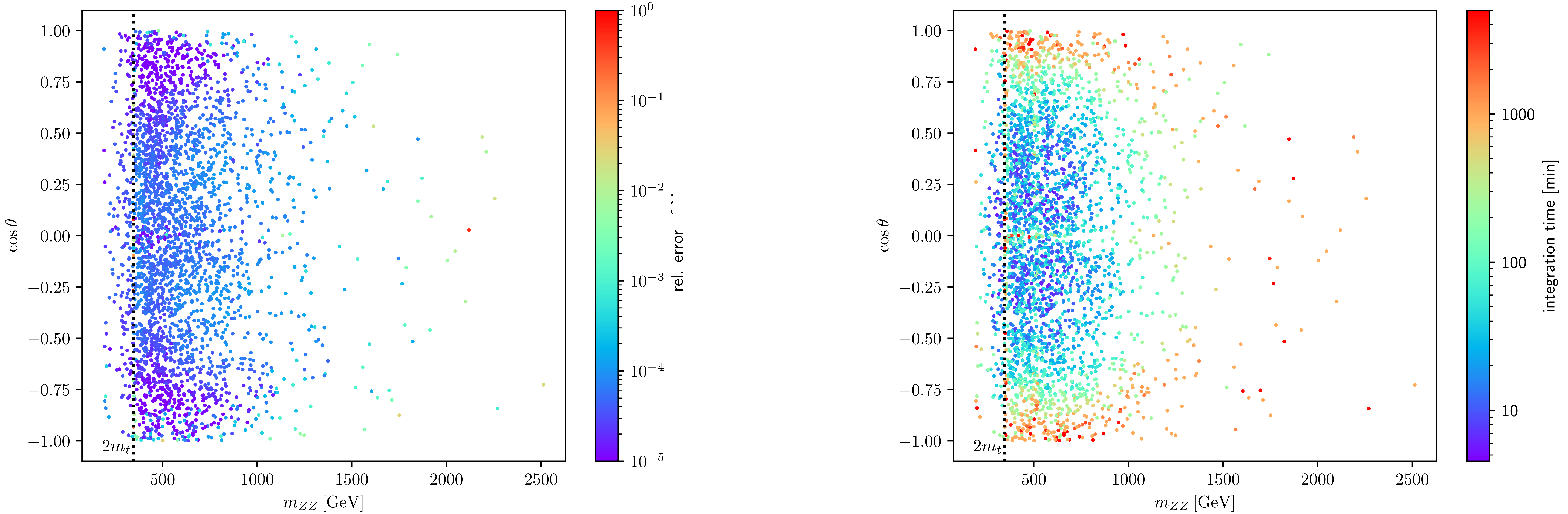

Numerical Evaluation

Good numerical stability in most regions of phase space, in particular around the top-quark threshold (except for small p_T)

Runtimes in $O(10)$ min for large part of the phase space with expected difficulties for very small p_T

Can access high energy and high p_T region without much difficulty, but very high energy $\left(\sqrt{s} > 2\,TeV\right)$ challenging

Better than per-mille precision for most of the phase-space

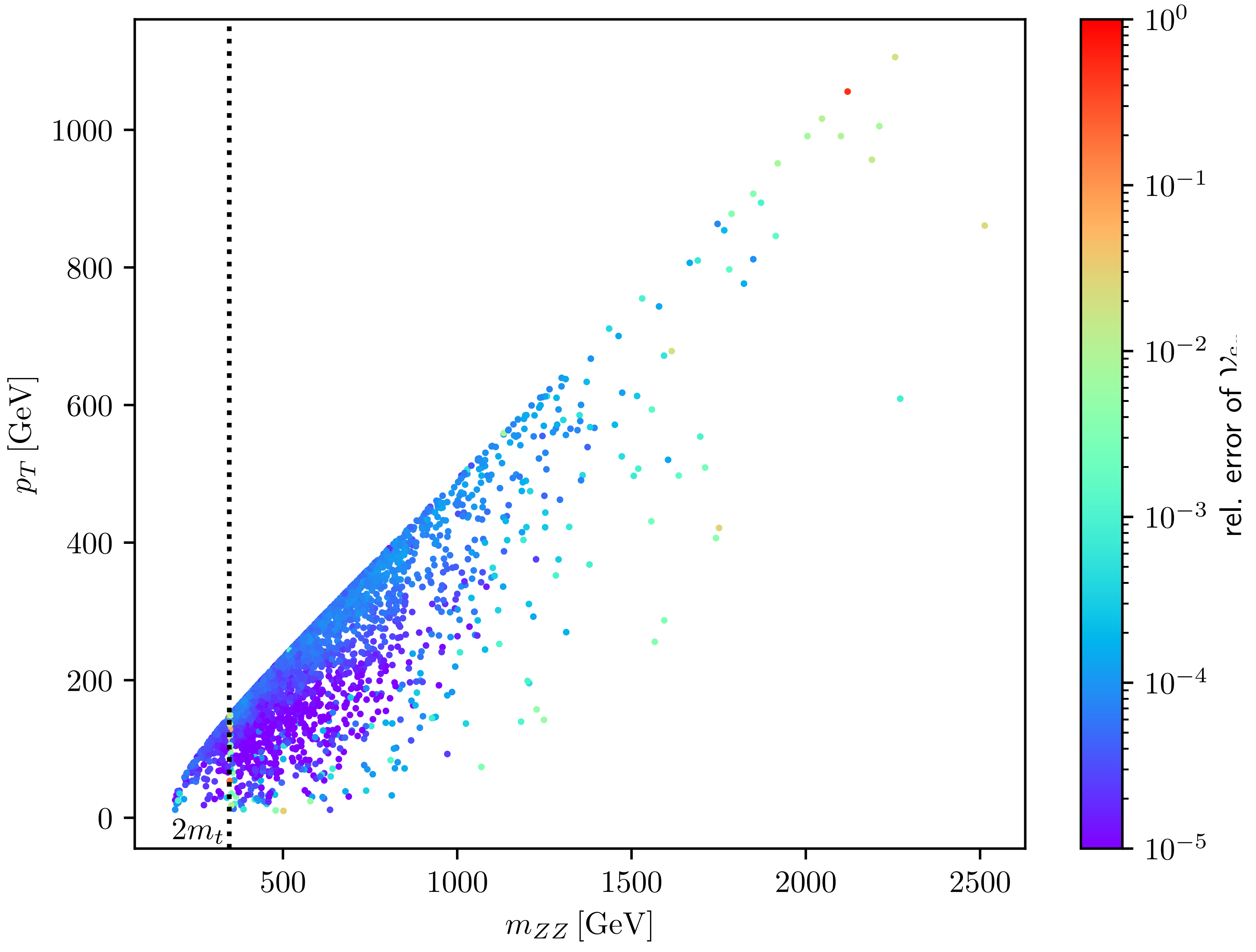

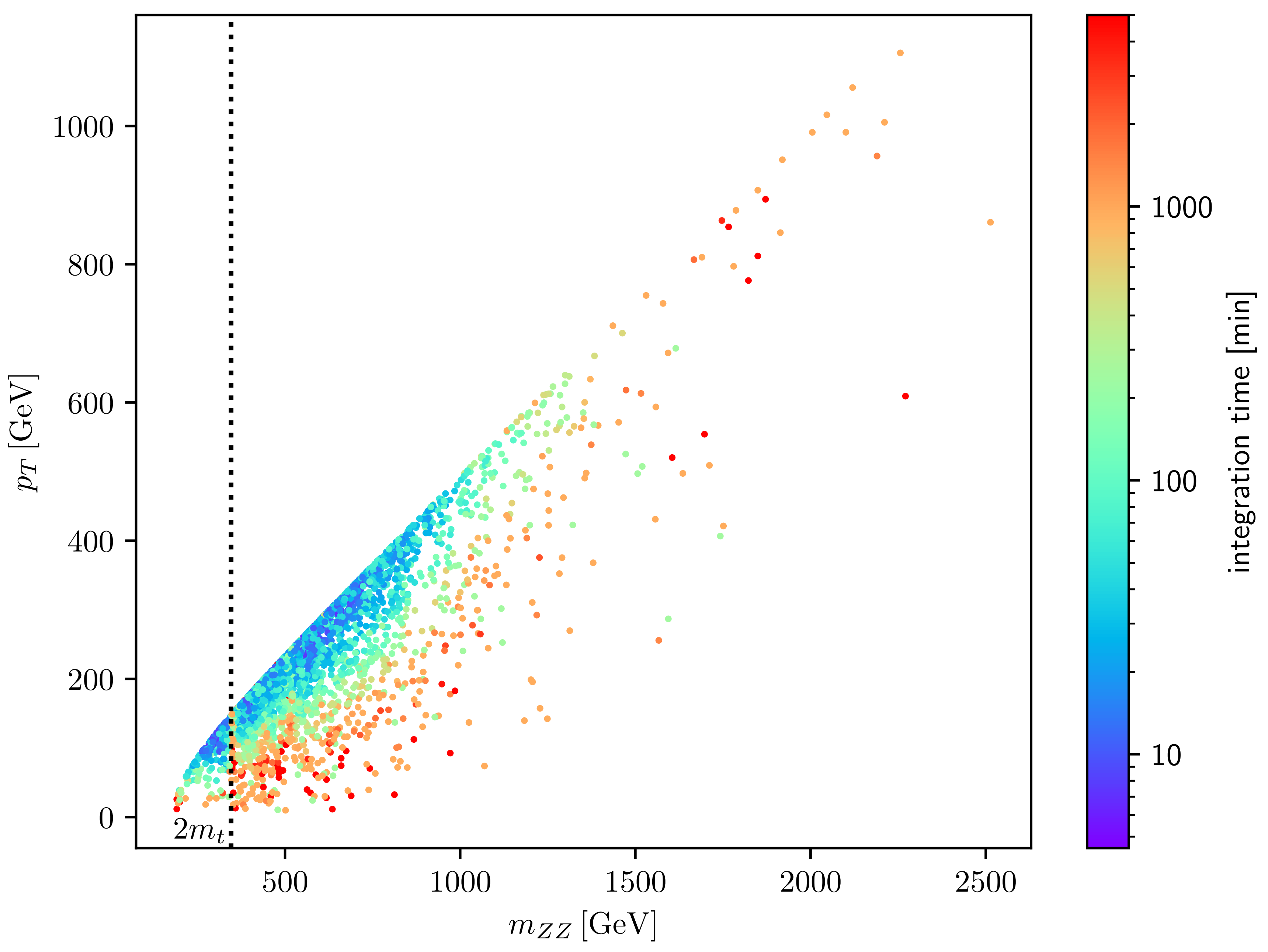

Comparison to expansions

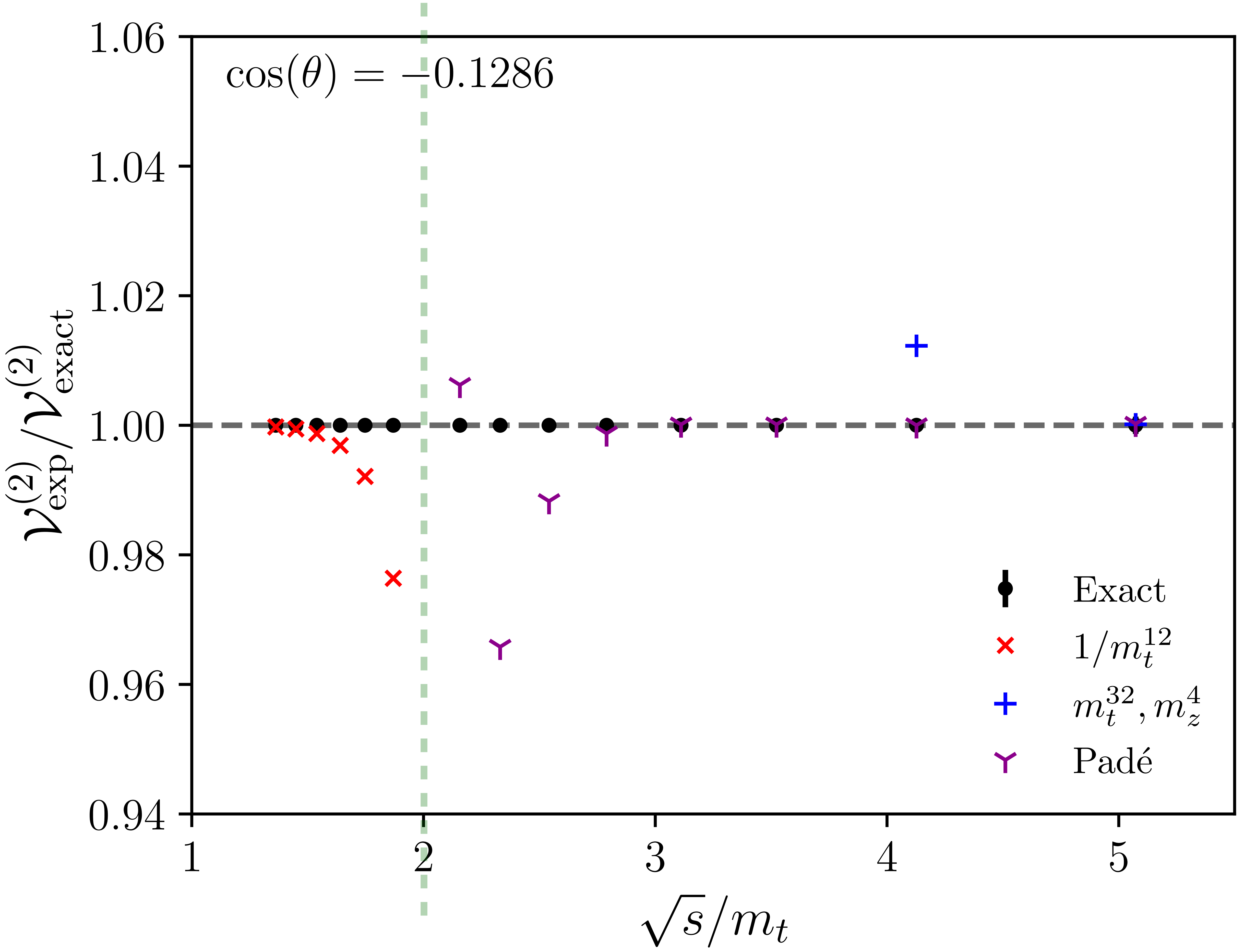

Comparison of $\sqrt{s}$ dependence of the unpolarised interference with expansion results at fixed $\cos\theta = -0.1286$. Exact results from [BA, Jones, von Manteuffel (2020)]. Expansion and Padé results from [Davies, Mishima, Steinhauser, Wellmann (2020)] (see also [Davies, Mishima, Schönwald, Steinhauser (2023)]). Error bars for the exact result are plotted but they are too small to be visible.

Comparison to expansions

Karlsruher Institut für Technologie

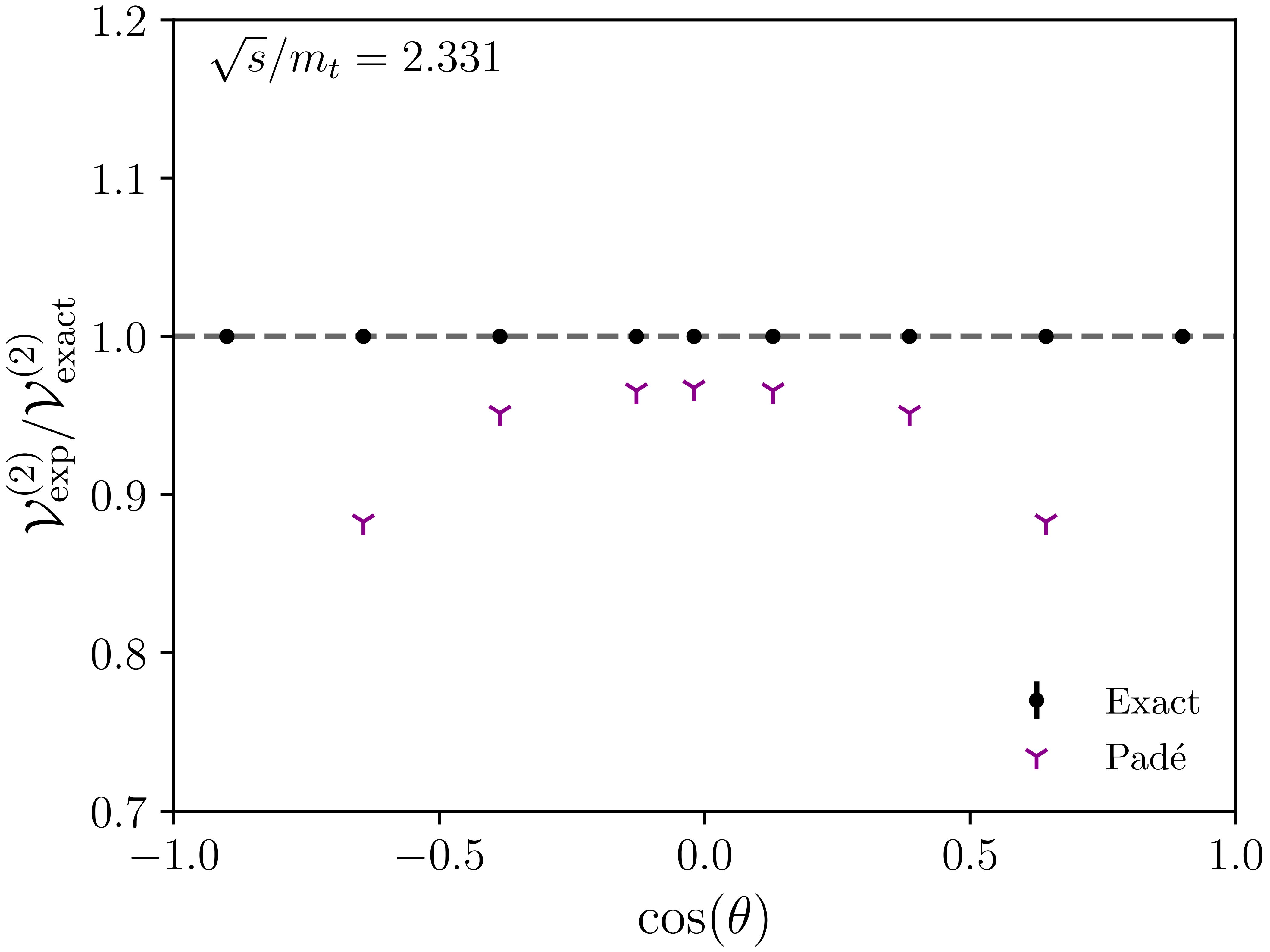

Comparison of $\cos\theta$ dependence of the unpolarised interference with expansion results at fixed energy $\sqrt{s} = 403$ GeV. Exact results from **[BA, Jones, von Manteuffel (2020)]**. Expansion and Padé results from [Davies, Mishima, Steinhauser, Wellmann (2020)] (see also [Davies, Mishima, Schönwald, Steinhauser (2023)]).

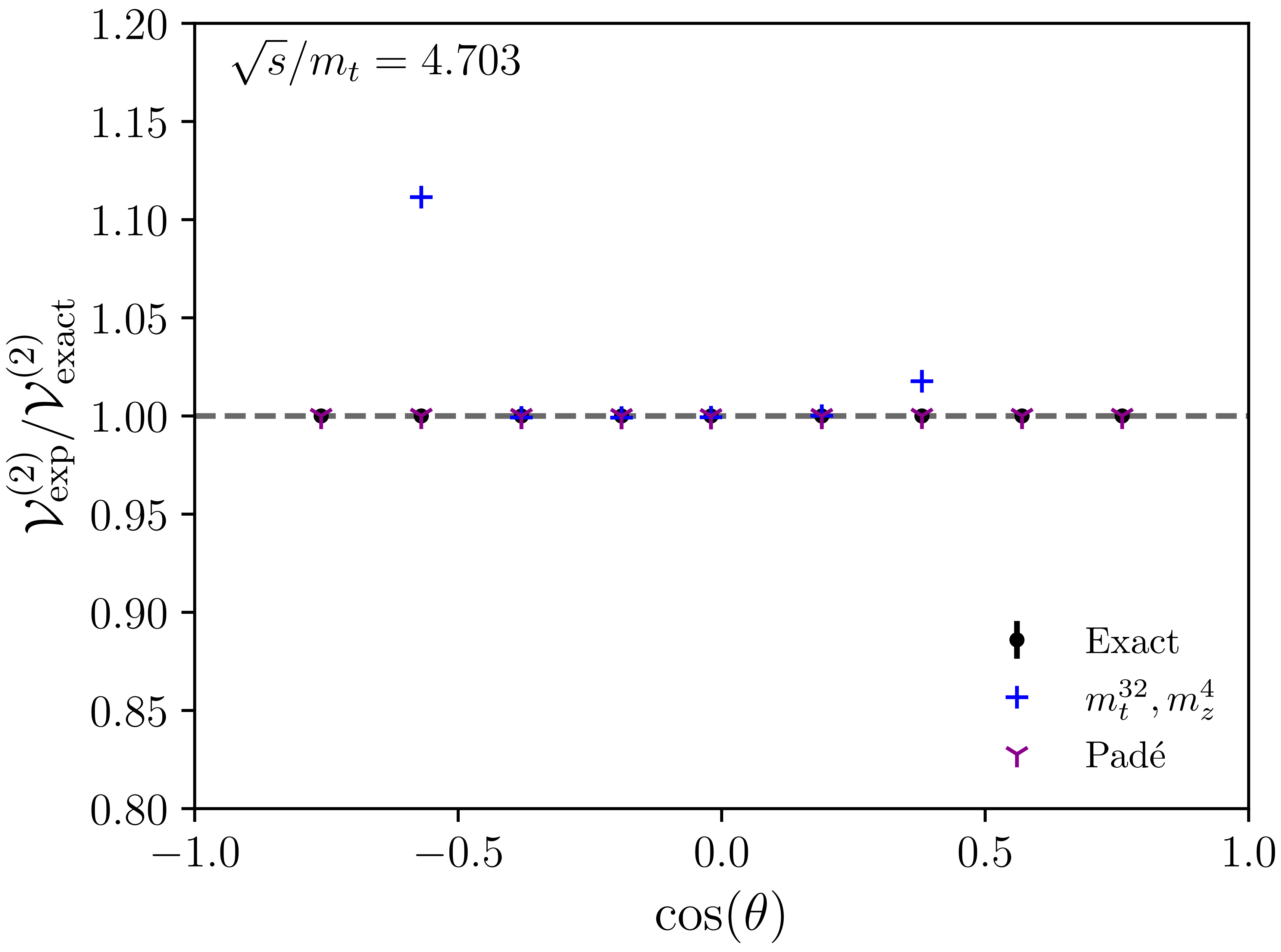

Comparison of $\cos\theta$ dependence of the unpolarised interference with expansion results at fixed energy $\sqrt{s} = 814$ GeV. Exact results from **[BA, Jones, von Manteuffel (2020)]**. Expansion and Padé results from [Davies, Mishima, Steinhauser, Wellmann (2020)] (see also [Davies, Mishima, Schönwald, Steinhauser (2023)]).

Comparison to expansions

Karlsruher Institut für Technologie

For previous results, "q_T" subtraction scheme

Transformation between Catani's original scheme and q_T scheme

$$A_i^{(2),fin,Catani} = A_i^{(2),fin,q_T} + \Delta I_1 A_i^{(1),fin}$$

$$\Delta I_1 = -\frac{1}{2}\pi^2 C_A + i\pi\beta_0 \quad \sim 15$$

For interference terms, 1-loop result multiplied by ~ 30 => Leads to a very different qualitative behaviour

Relative comparisons highly dependent on IR scheme

Comparison to expansions

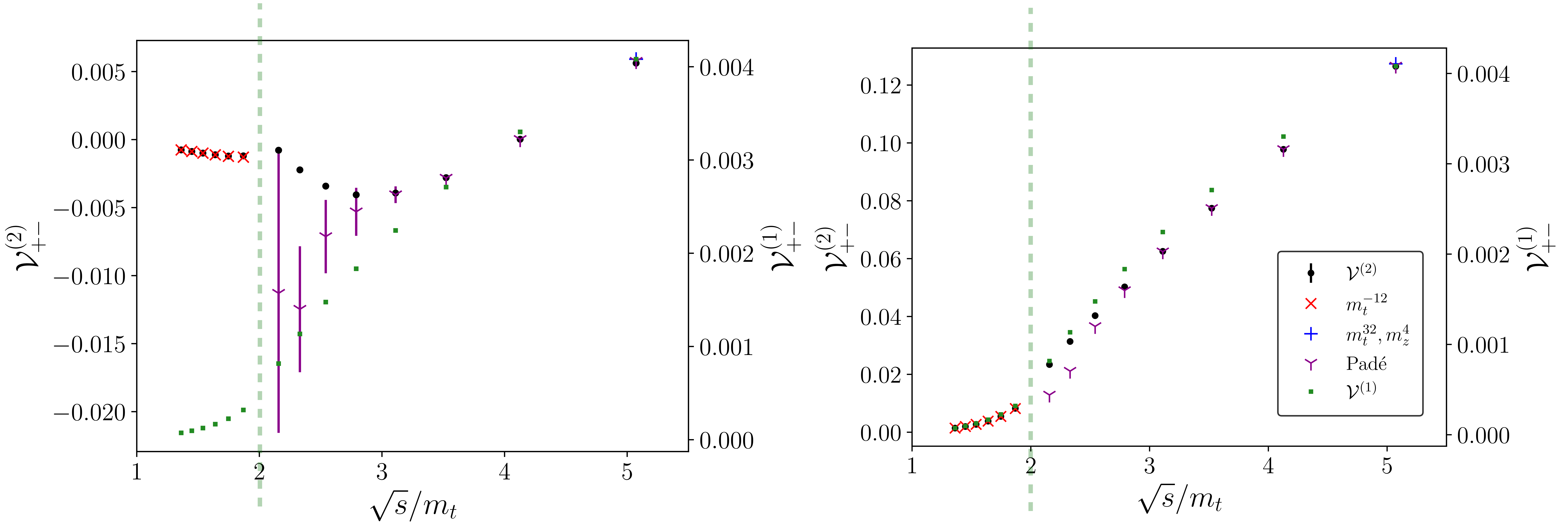

Traditional Catani Scheme

"q_T" scheme

Comparison of $\sqrt{s}$ dependence of the polarised interference with expansion results at fixed $\cos\theta = -0.1286$. Exact results from **[BA, Jones, von Manteuffel (2020)]**. Expansion and Padé results from [Davies, Mishima, Steinhauser, Wellmann (2020)] (see also [Davies, Mishima, Schönwald, Steinhauser (2023)]).

Comparison to expansions

Karlsruher Institut für Technologie

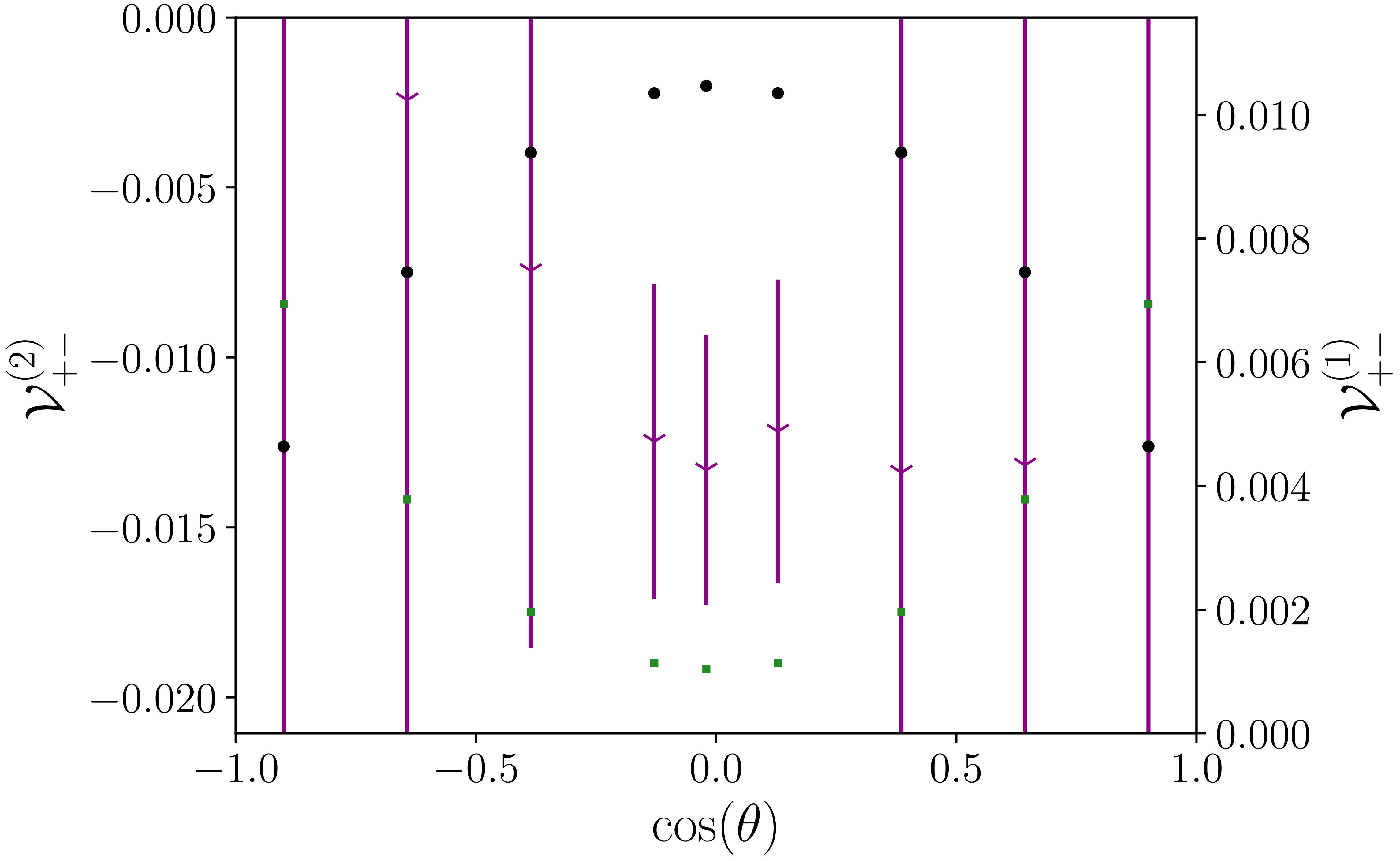

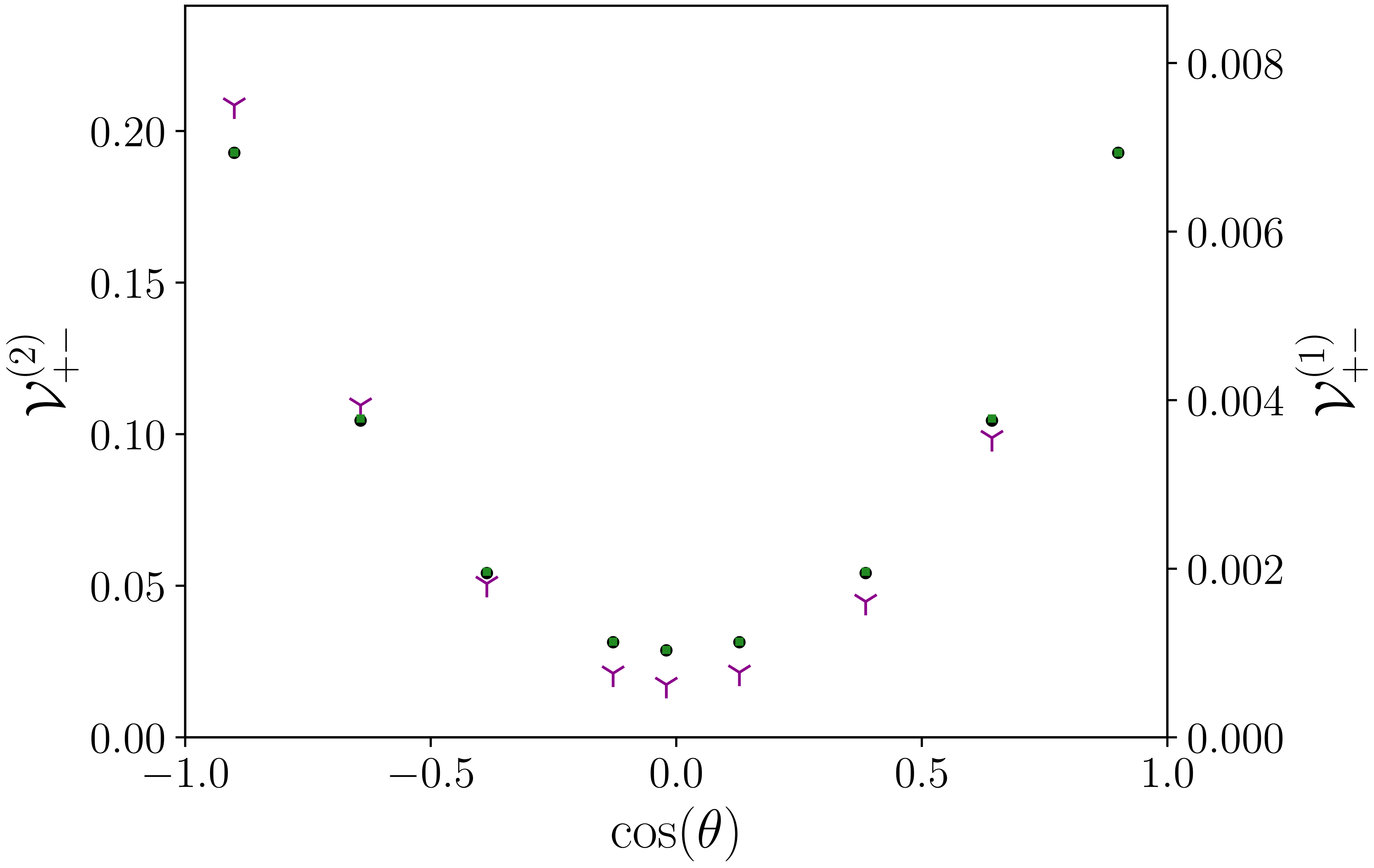

Traditional Catani Scheme

"q_T" scheme

Comparison of $\cos\theta$ dependence of the polarised interference with expansion results at fixed $\sqrt{s}/m_t = 2.331$. Exact results from **[BA, Jones, von Manteuffel (2020)]**. Expansion and Padé results from [Davies, Mishima, Steinhauser, Wellmann (2020)] (see also [Davies, Mishima, Schönwald, Steinhauser (2023)]).

Higgs and Top quark

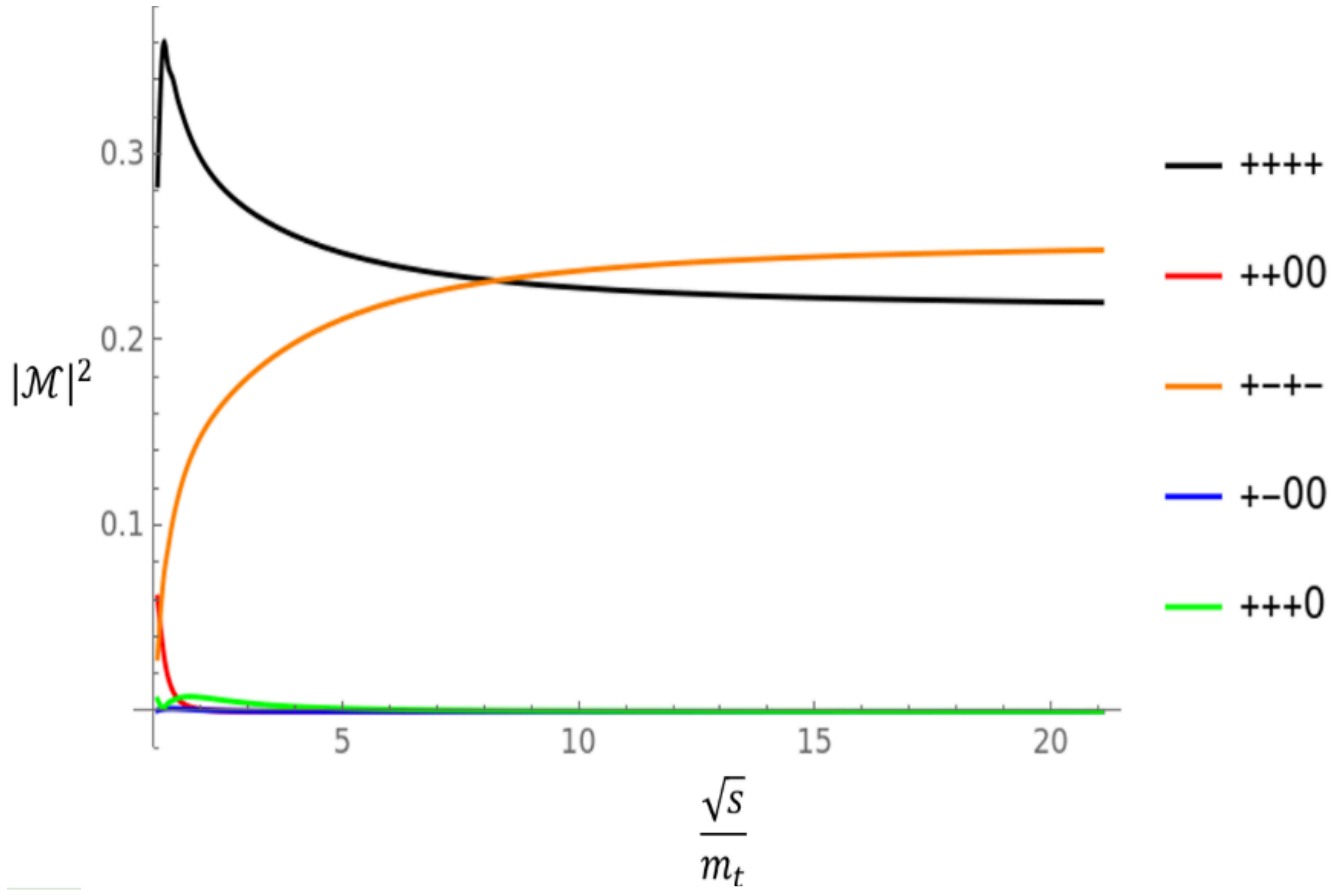

Comparison of Born $|\mathscr{M}|^2$ against $\sqrt{s}$ for different helicity contributions for massless quarks

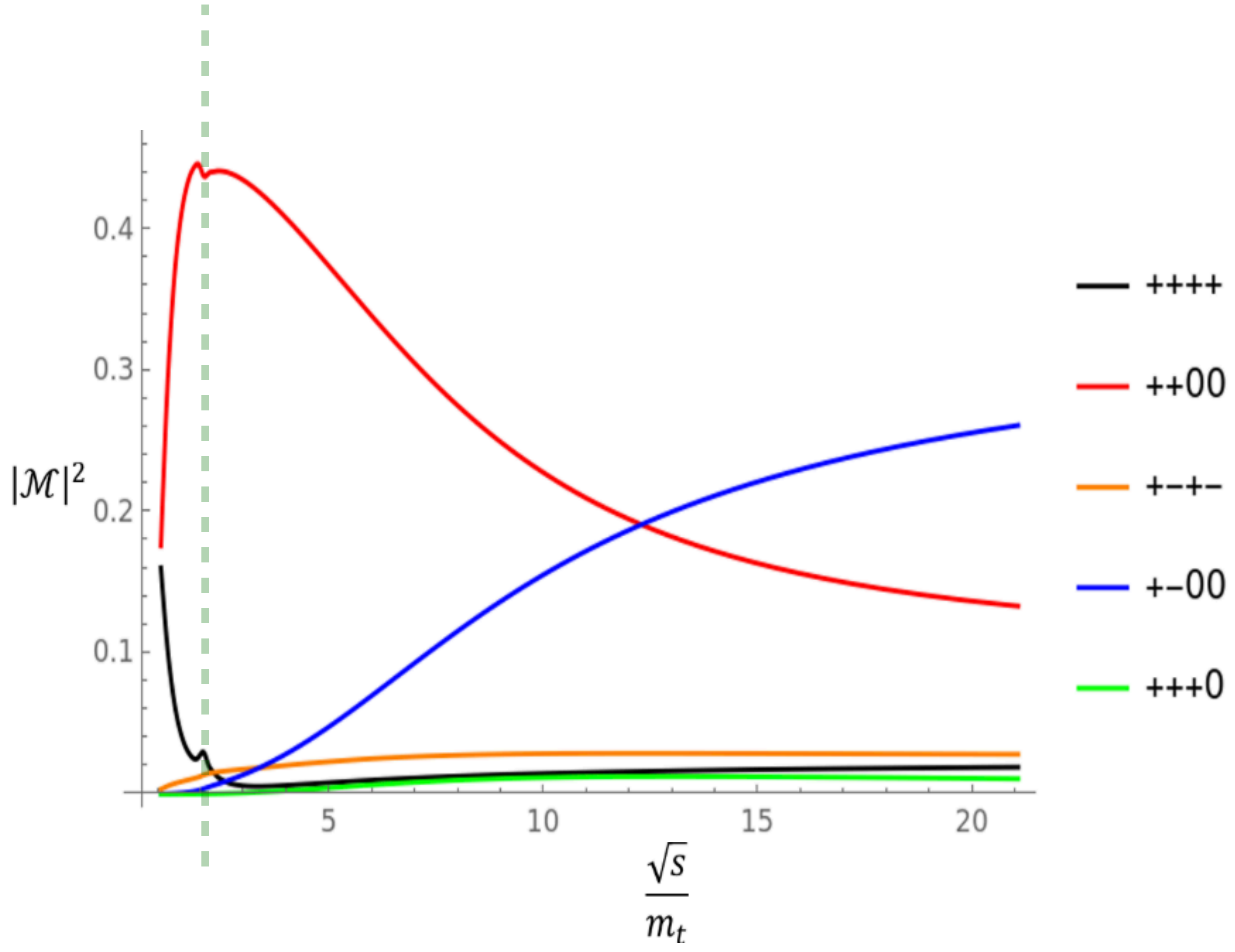

Comparison of Born $|\mathscr{M}|^2$ against $\sqrt{s}$ for different helicity contributions for massive (including Higgs) quarks

Higgs and Top quark

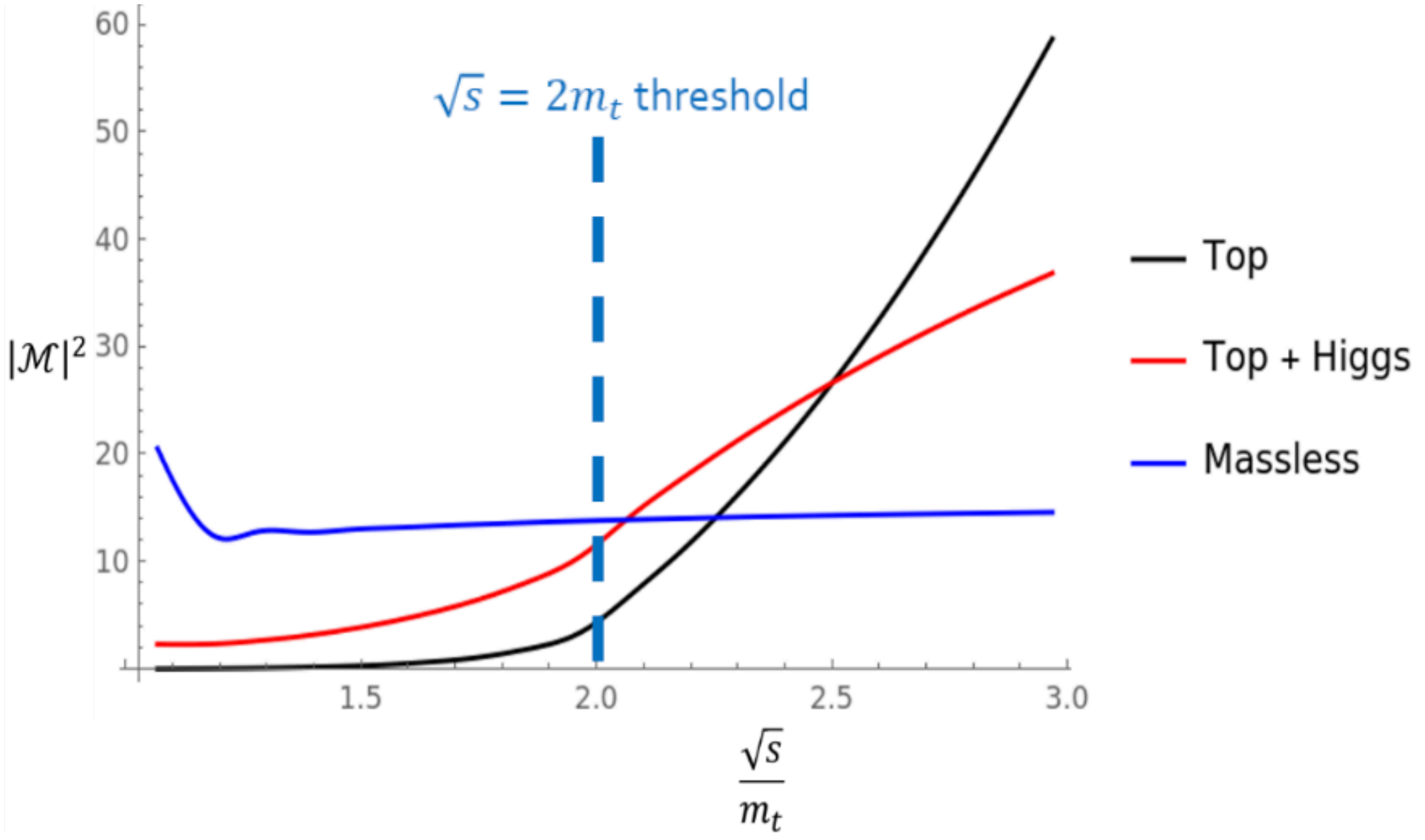

Comparison of Born $|\mathcal{M}|^2$ against $\sqrt{s}$ for different contributions

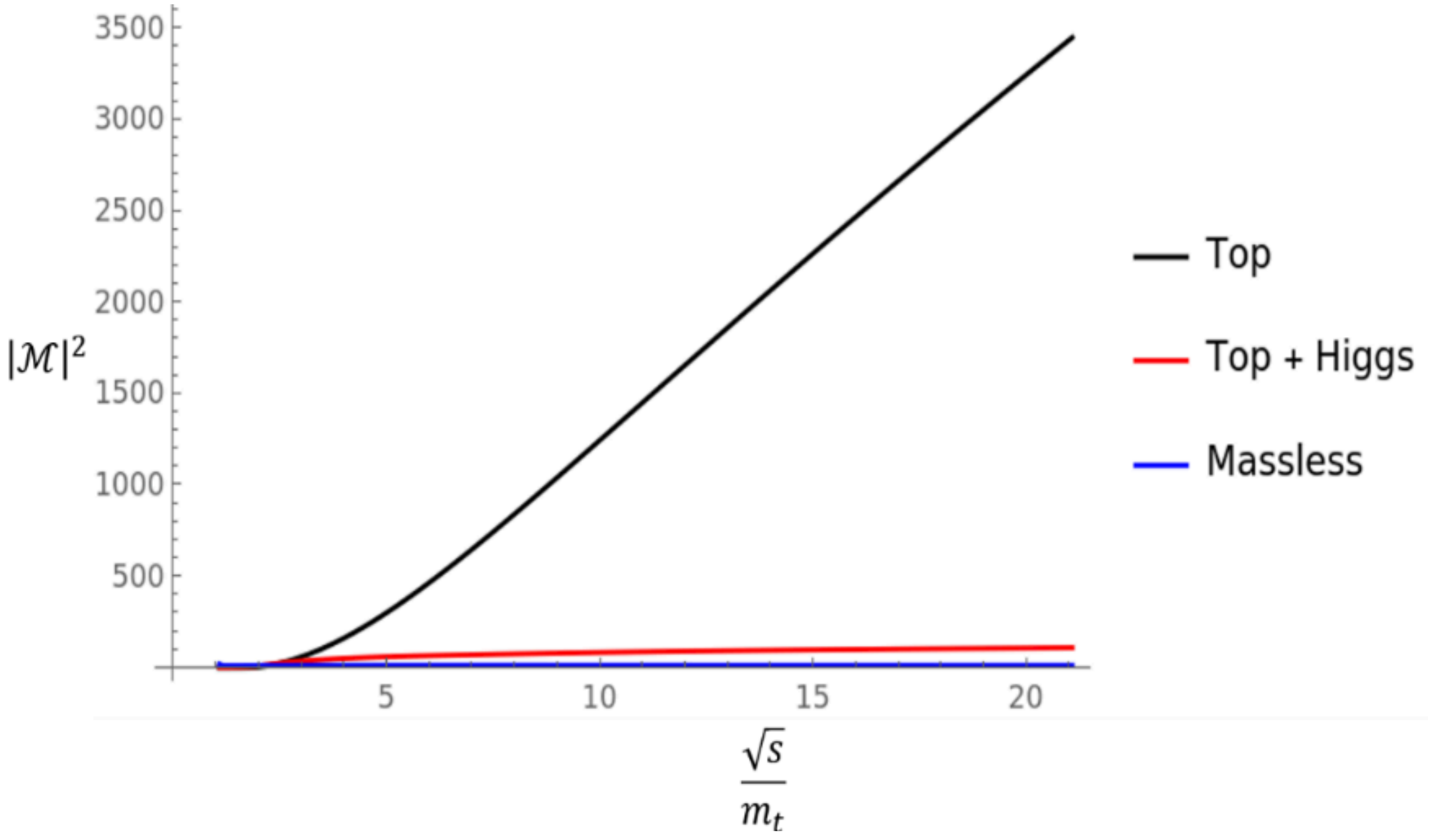

Comparison of Born $|\mathcal{M}|^2$ against $\sqrt{s}$ for different contributions at very high energies

Higgs and Top quark

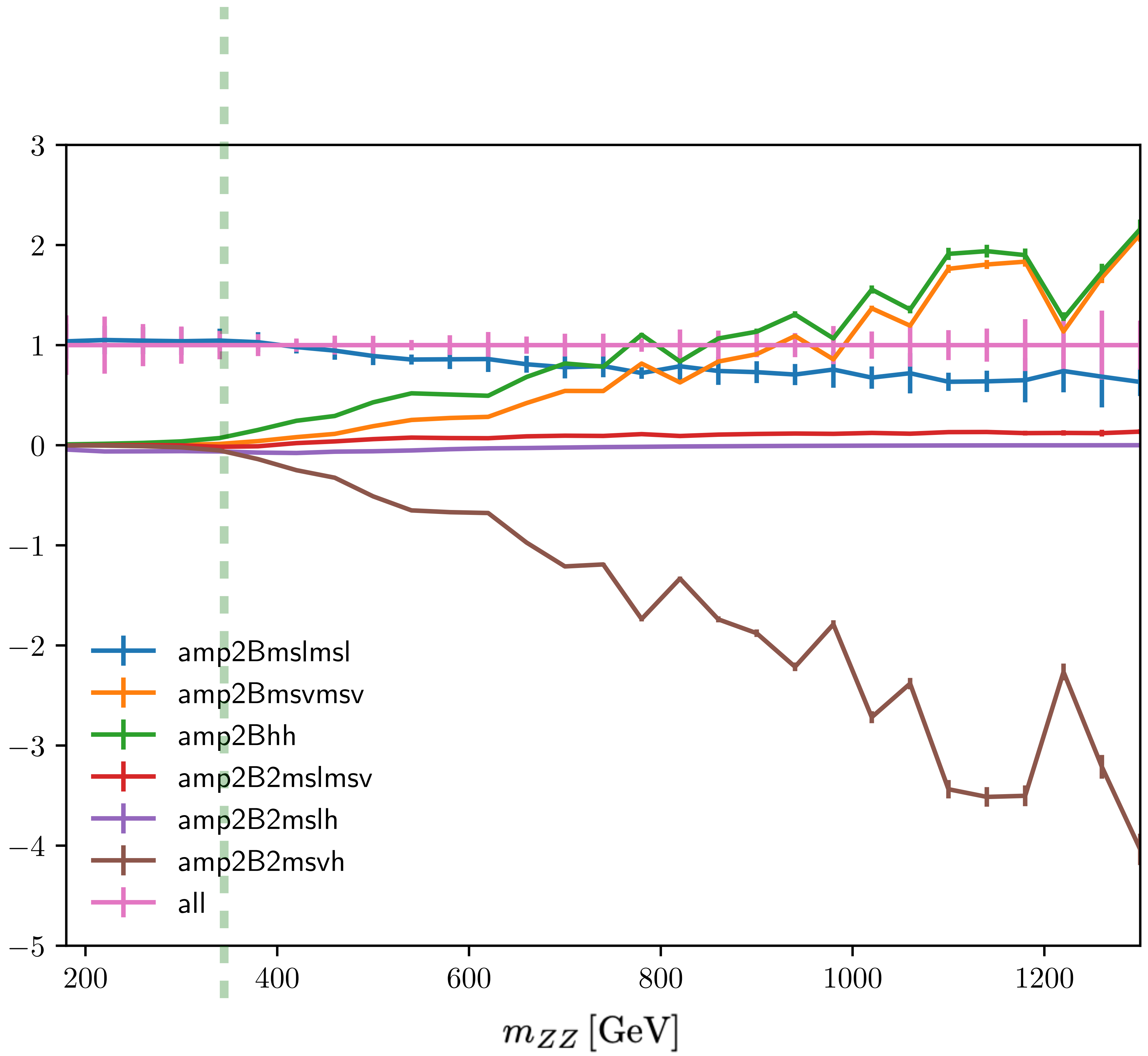

Comparison of ratios of different interferences (normalised to full) at 1-loop level against m_{ZZ}

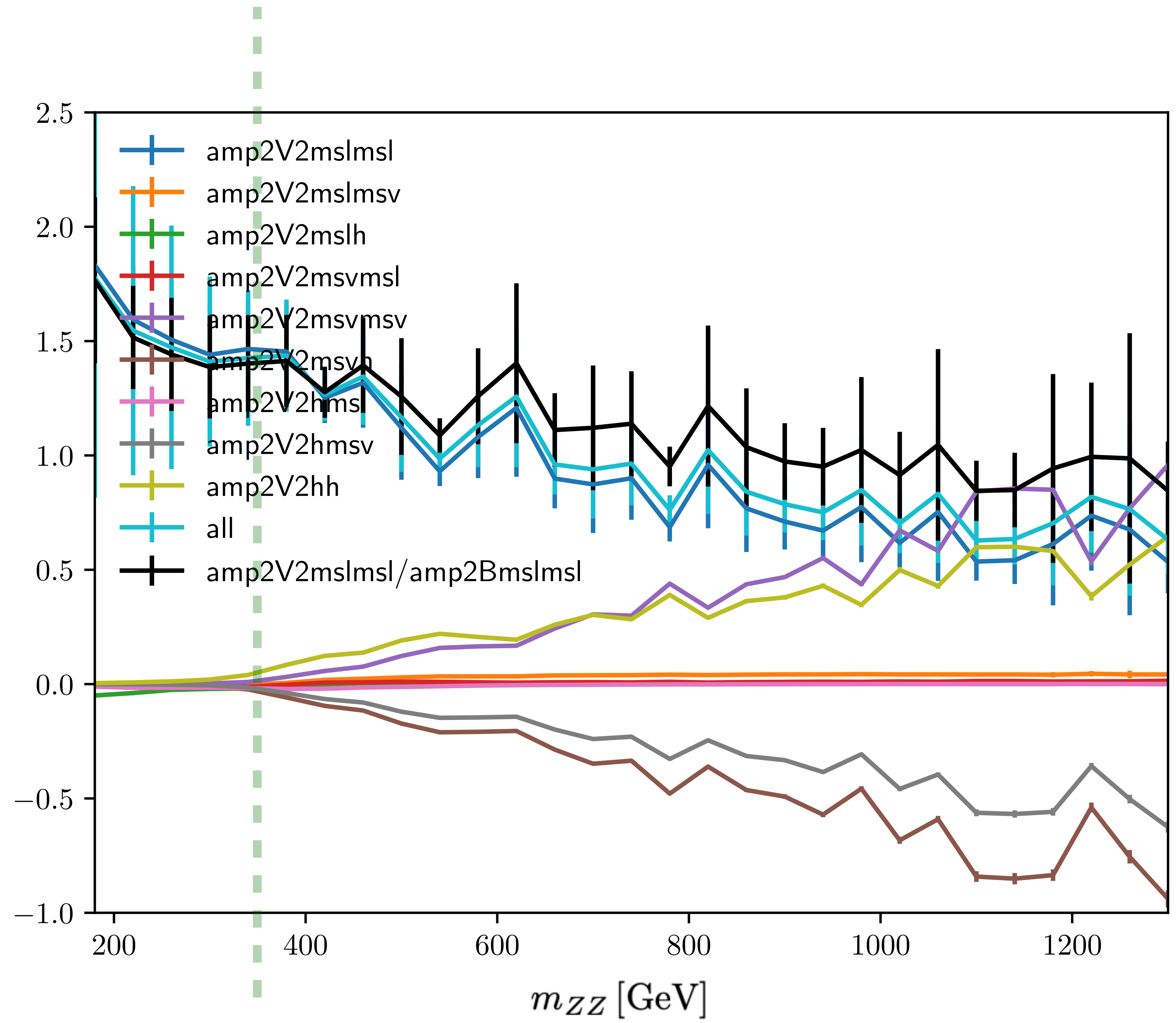

Comparison of ratios of different interferences (normalised to full) at 2-loop level against m_{ZZ}

Higgs and Top quark

Karlsruher Institut für Technologie

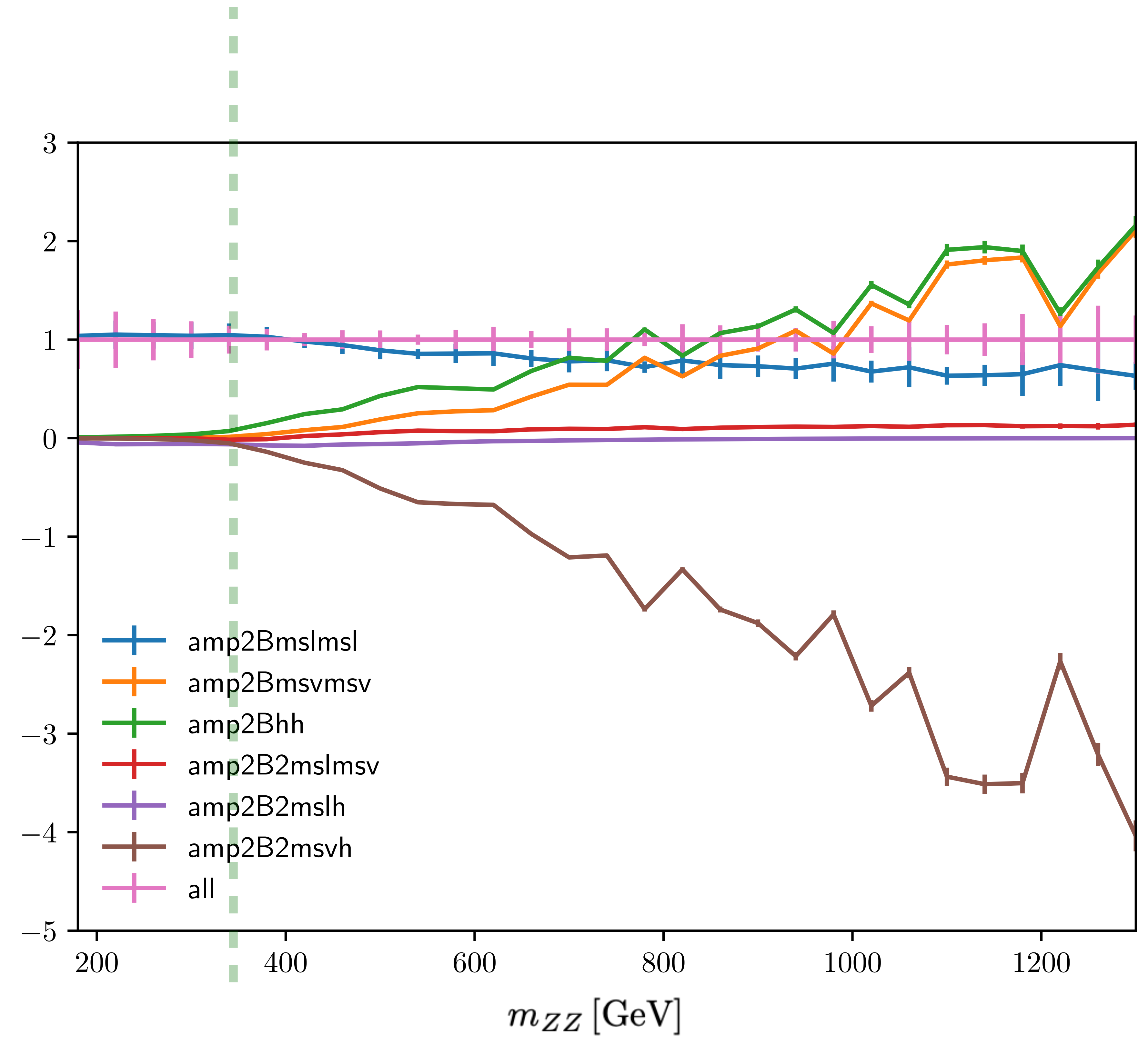

Comparison of ratios of different interferences (normalised to full) at 1-loop level against m_{ZZ}

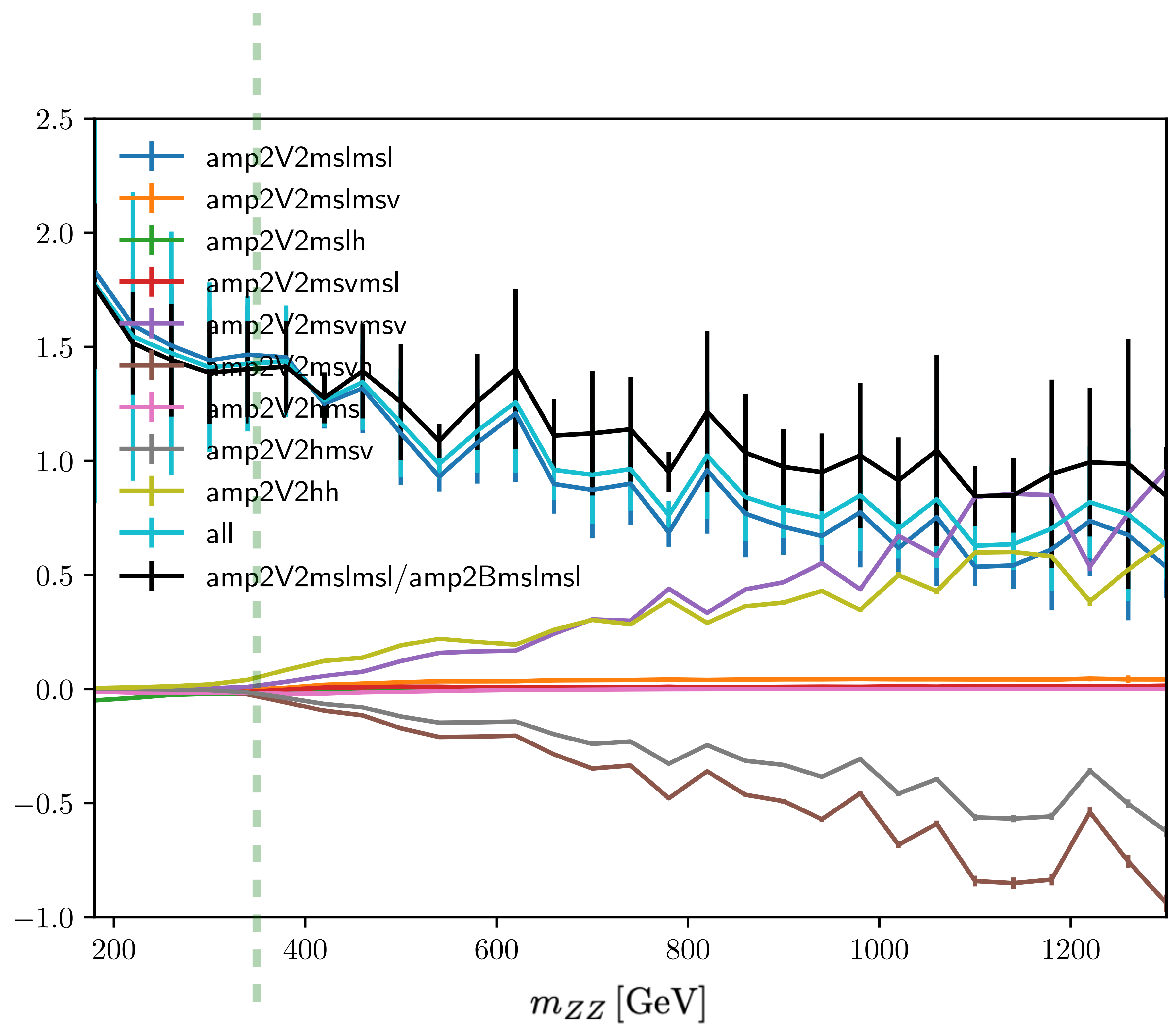

Comparison of ratios of different interferences (normalised to full) at 2-loop level against m_{ZZ}

Delicate cancellations between top-only and Higgs mediated contributions

Results: Complete NLO Corrections

Top-only contributions:

$$\sigma_{\mathrm{LO}}^{\mathrm{A}_h} = 19.00^{+29.4\%}_{-21.4\%}\ \mathrm{fb}$$

$$\sigma_{\mathrm{NLO}}^{\mathrm{A}_h} = 34.46(6)^{+16.4\%}_{-14.4\%}\ \mathrm{fb}$$

Including all contributions:

$$\sigma_{\mathrm{LO}} = 1316^{+23.0\%}_{-18.0\%}\ \mathrm{fb}$$

$$\sigma_{\mathrm{NLO}} = 2275(12)^{+14.0\%}_{-12.0\%}\ \mathrm{fb}$$

(Number in parentheses indicates the Monte-carlo error)

~2% decrease in full NLO cross-section after including top quark and Higgs contributions

Results: Complete NLO Corrections

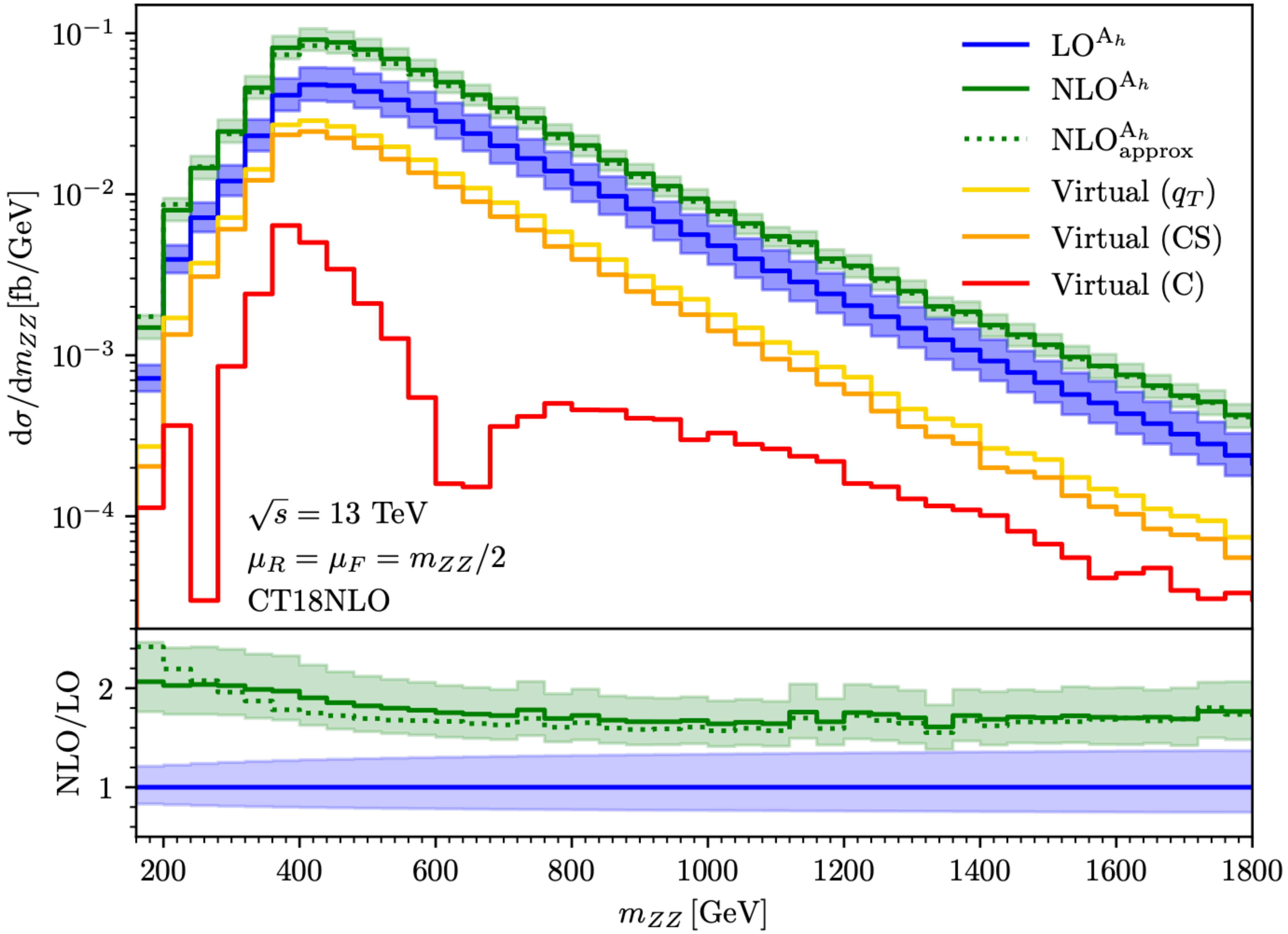

Top-quark-only contributions to the ZZ invariant mass distribution in pp collisions. The absolute value of the two-loop virtual correction is shown separately in the qT , Catani-Seymour (CS), and Catani (C) schemes. The dashed curve represents an approximate NLO result obtained by rescaling the massive Born amplitude with the massless K-factor.

Plot from [BA, Jones, Kerner, von Manteuffel (2024)]

Results: Complete NLO Corrections

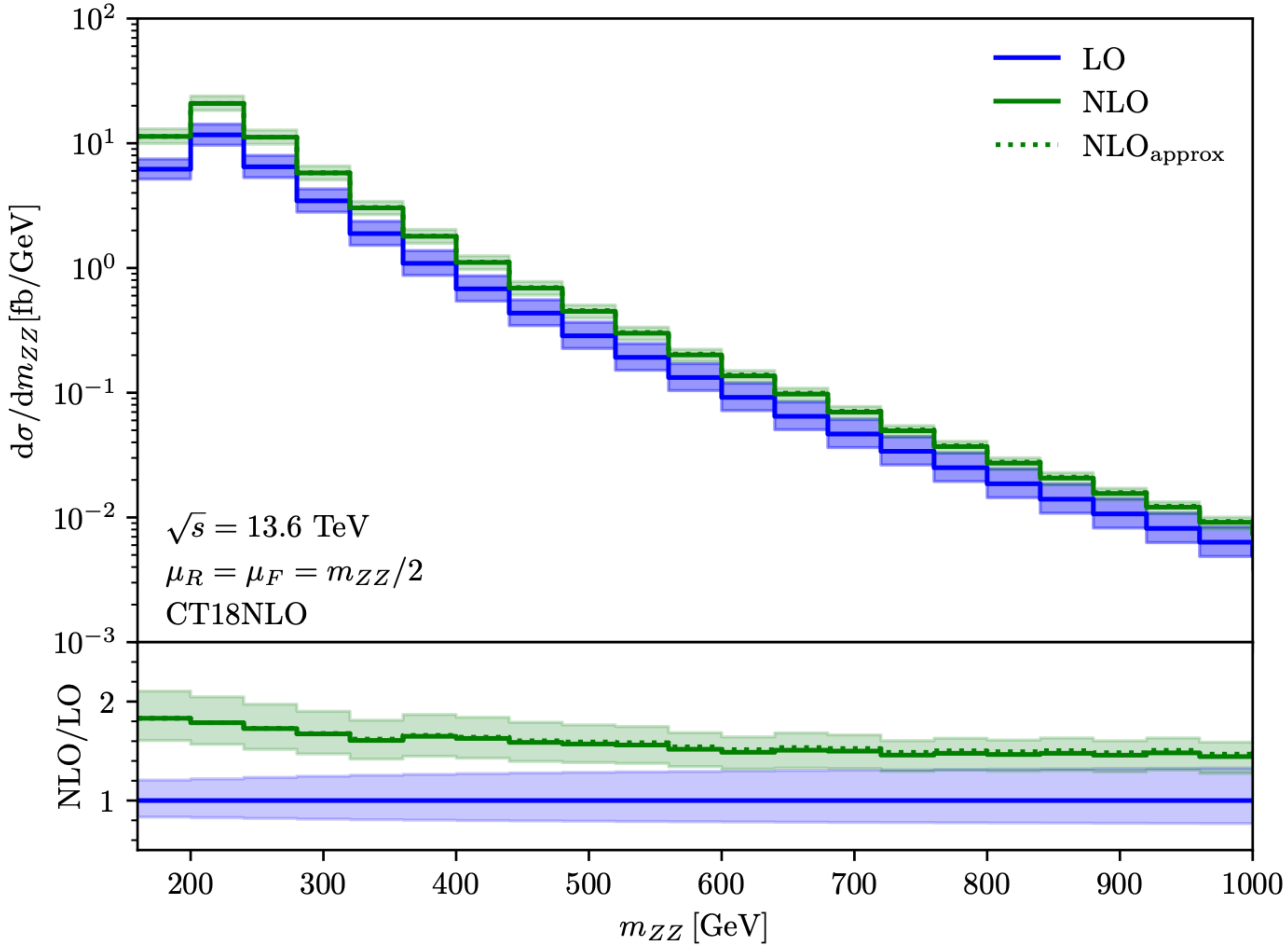

Diboson invariant mass distribution for gluon- initiated ZZ production at the LHC. The Solid curves represent the LO and NLO results with complete massless and massive contributions, including Higgs-mediated diagrams. The dashed curve represents an approximate NLO result obtained as described in the text. Plot from **[BA, Jones, Kerner, von Manteuffel (2024)]**

Top mass scheme uncertainty

Karlsruher Institut für Technologie

We can estimate the mass uncertainty by comparing the numbers between on-shell and $\overline{\text{MS}}$ schemes. For $\overline{\text{MS}}$ scheme, we use $m_t(2m_t) = 154.6\ \text{GeV}$

At Leading Order:

$$\sigma_{LO}^{OS} = 19.00\ \text{fb}$$

$$\sigma_{LO}^{\overline{MS}} = 20.89\ \text{fb} \qquad \implies \sim 10\,\%\ \text{increase}$$

At NLO, we can estimate the uncertainty by varying everything except the finite 2-loop amplitudes, which are not available with symbolic top mass dependence.

	OS	MS	Ratio
Born	19.00	20.89	1.099
Reals (Catani)	14.89	16.33	1.097
Reals (qT)	5.80	6.22	1.07
Virtuals (Catani)	0.59	?	

However, the impact of these finite 2-loop amplitudes can be reduced by working in Catani scheme to get a better estimate (In progress).

Conclusions

Two-loop amplitudes

Efficient integration strategy using sector decomposition to minimise the total integration time; able to get good statistics for distributions

Numerically very stable in most regions of phase-space, even close to top-quark pair production threshold, at high invariant mass and forward scattering

NLO corrections

Significant top-quark only corrections (~100%)

Great impact due to the choice of IR scheme on virtual (and reals)

Existing approximations based on rescaling the massive Born by massless k-factor quite good for unpolarised cross-section

Extreme cancellations between Higgs and Top-quark contributions; sensitive to exact SM couplings